ADVANCING EARTH AND SPACE SCIENCES

Tectonics

RESEARCH ARTICLE
10.1029/2026TC009430

Structural Evolution of the Gaggiano High: A Preserved Rift-Related Structural High in the Western Po Plain (Italy)

M. Mercuri[1], L. Spaggiari[2], A. P. Amodio[2], S. Bigi[1], A. Corrao[2], C. Doglioni[1], F. Trippetta[1], and E. Carminati[1]

[1]Dipartimento di Scienze della Terra, Sapienza Università di Roma, Roma, Italy, [2]Eni, San Donato Milanese, Italy

Key Points:

- 3D seismic data reveal a well-preserved Triassic–Jurassic rift-related structural high in the Western Po Plain
- Throw–distance analysis shows that most displacement accumulated during early Mesozoic extension, with minor Paleogene reactivation
- Rift inheritance controlled deformation partitioning and limited inversion during Alpine–Apennine contraction

Supporting Information:

Supporting Information may be found in the online version of this article.

Correspondence to:

M. Mercuri,
marco.mercuri@uniroma1.it

Citation:

Mercuri, M., Spaggiari, L., Amodio, A. P., Bigi, S., Corrao, A., Doglioni, C., et al. (2026). Structural evolution of the Gaggiano High: A preserved rift-related structural high in the Western Po Plain (Italy). *Tectonics*, *45*, e2026TC009430. https://doi.org/10.1029/2026TC009430

Received 19 FEB 2026
Accepted 20 JUN 2026

Author Contributions:

Conceptualization: M. Mercuri, E. Carminati
Data curation: M. Mercuri
Formal analysis: M. Mercuri
Funding acquisition: M. Mercuri, E. Carminati
Investigation: M. Mercuri
Methodology: M. Mercuri, L. Spaggiari, A. P. Amodio, A. Corrao
Project administration: M. Mercuri, L. Spaggiari, E. Carminati
Resources: L. Spaggiari, A. P. Amodio, A. Corrao
Supervision: L. Spaggiari, E. Carminati
Validation: S. Bigi, C. Doglioni, F. Trippetta, E. Carminati
Visualization: M. Mercuri
Writing – original draft: M. Mercuri

Abstract The Gaggiano High, buried beneath the sediments of the Western Po Plain (northern Italy), represents one of the few examples of Mesozoic structural highs largely preserved within a foreland–foredeep system. Unlike the adjacent Lacchiarella Basin, which underwent strong positive inversion during the Neogene, the Gaggiano High experienced only mild contractional reactivation, allowing its original extensional framework to be preserved. By integrating 3D seismic interpretation, isochore maps, and well data, we reconstruct the tectono-stratigraphic evolution of the Gaggiano High from Middle Triassic rifting to Neogene burial. Isochore maps and stratigraphic geometries reveal major thickness variations and westward tilting along N-S faults during Early to Middle Jurassic extension, followed by long-lasting structural uplift and reduced sedimentation during Jurassic-Cretaceous times. In the Paleogene, renewed extension along NW–SE faults produced local depocentres within the Scaglia Fm., while subsequent Oligo-Miocene compression resulted in gentle folding, minor inversion of inherited normal faults, and regional tilting. Comparison with the exhumed Lugano Swell highlights the long-term persistence of rift-related highs as mechanically rigid domains within evolving foreland basins. The Gaggiano High thus provides a well-preserved subsurface analogue illustrating how inherited normal faults and long-lived structural highs may constrain, modulate, or even inhibit subsequent deformation, stratigraphic architecture and basin evolution across the Alpine-Apennine system.

Plain Language Summary Mountain belts commonly develop on top of older geological structures formed during earlier phases of continental stretching. These inherited structures can strongly influence how later compression is distributed, but they are often difficult to reconstruct because they are heavily overprinted by deformation. In this study, we investigate the Gaggiano High, a buried geological structure beneath the Po Plain in northern Italy. Using three-dimensional seismic reflection data and well information, we reconstruct its tectonic evolution from Middle Triassic continental rifting to Neogene burial beneath Alpine and Apennine sediments. Our results show that the Gaggiano High formed as a tilted fault block during early Mesozoic extension and remained a topographic and structural high for over 100 million years. Quantitative analysis of fault displacement demonstrates that most movement occurred during Triassic–Early Jurassic rifting, whereas later Paleogene and Neogene tectonic phases only slightly reactivated the inherited faults. Unlike nearby structures that underwent strong inversion during mountain building, the Gaggiano High largely preserved its original extensional architecture. This case study provides a clear subsurface example of how ancient rift-related fault systems can persist through multiple tectonic cycles and influence the spatial distribution of deformation in foreland basin settings.

1. Introduction

Inherited paleogeographic features—particularly rift-related structural highs—exert a first-order control on deformation style, stratigraphic architecture, and resource distribution during subsequent tectonic phases (e.g., Butler et al., 2006; Lescoutre & Manatschal, 2020; Tavani et al., 2021). Inherited rift-related highs represent rigid domains that may either localize or inhibit later shortening, influencing the development of foreland and foredeep system where advancing orogenic fronts may preserve or reactivate pre-existing extensional structures (e.g., Sieberer et al., 2023).

In the peri-Adriatic region, such highs developed mainly during the Triassic to Early Jurassic rift-related events (Berra & Carminati, 2010; Bertotti et al., 1993; Bosellini, 1973). Their structural inheritance profoundly affected the subsequent Alpine and Apennine deformation (Butler et al., 2006). Yet, most rift-related highs are strongly overprinted by contractional deformation, both in the Alps (e.g., Mohn et al., 2011; Schönborn, 1992; Zanchi

Writing – review & editing: M. Mercuri, L. Spaggiari, S. Bigi, F. Trippetta, E. Carminati

et al., 2012) and in the Apennines (e.g., Cardello & Doglioni, 2015; Pace et al., 2015; Tavarnelli et al., 2004), hampering the reconstruction of their tectono-stratigraphic evolution.

The Western Po Plain is the foreland of both Alps and Apennines and provides an opportunity to investigate such inherited structures in the subsurface. In this area, Mesozoic extensional highs and lows formed along the Adria passive margin are now buried beneath a thick Neogene cover but retain key elements of their original geometry (Fantoni et al., 2004; Turrini et al., 2016, 2018). Among these, the Gaggiano High stands out as a well-preserved Mesozoic structural high that experienced only mild Neogene inversion, in contrast to the adjacent Lacchiarella area, which underwent strong positive inversion (Fantoni et al., 2004).

In this study, we integrate 3D seismic interpretation, isochore maps, and well data to reconstruct the multiphase tectono-stratigraphic evolution of the Gaggiano High, whose Mesozoic extensional architecture is remarkably preserved despite subsequent Cenozoic tectonic phases, from Middle Triassic syn-rift extension to Neogene contraction. By comparing the buried Gaggiano High with the exhumed Lugano Swell in the western Southern Alps, we discuss the long-term persistence of inherited rift-related structures and their mechanical role in controlling foreland basin evolution across the Alpine-Apennine system.

2. Geological Setting

2.1. Regional Framework: The Western Po Plain

The Gaggiano structure lies beneath the Western Po Plain, at the structural boundary between the buried fronts of the Central Southern Alps and the Northern Apennines (Figure 1a). This region represents a foreland-foredeep system developed in response to the convergence between the Eurasian plate and the Adria microplate, a promontory of the African plate (Carminati & Doglioni, 2012; Dercourt et al., 1986). Since the Cretaceous, this interaction has diachronously produced two opposite-verging orogenic belts: the south-verging Southern Alps (active since the Cretaceous; Zanchetta et al., 2012) and the northeast-verging Northern Apennines (since the Eocene-Oligocene, e.g., Carminati et al., 2012). The combined flexural load of the Alps and Apennines subduction zones generated the Neogene Po Plain basin, which simultaneously acts as the foredeep of the two orogenic belts (Cuffaro et al., 2010; Handy et al., 2010; Turrini et al., 2014).

Within this double-verging setting, Mesozoic extensional structures of the Adria passive margin are variably preserved or reactivated beneath the Cenozoic-Quaternary cover (Cassano, 1986; Fantoni & Franciosi, 2010; Mariotti & Doglioni, 2000; Pieri & Groppi, 1981; Turrini et al., 2014). The Gaggiano High represents one of these preserved structural highs, originally developed during Mesozoic rifting and later only mildly affected by Alpine-Apennine compression. This structure is part of the Gaggiano-Lacchiarella system, that constitutes one of the most prominent buried Mesozoic fault zones in the Po Plain (Figure 1a). It developed as a ~N-S-striking array of east-dipping normal faults that accommodated differential subsidence between an uplifted structural high (Gaggiano) and its adjacent depocentre (the Lacchiarella basin) (Fantoni et al., 2004; Turrini et al., 2016, 2018).

2.2. Rift- and Drift-Related Tectonics (Triassic-Jurassic)

During the Mesozoic, the Western Po Plain formed part of the passive continental margin of Adria, established during the breakup of Pangea (Bertotti et al., 1993; Castellarin et al., 1992; Winterer & Bosellini, 1981). The regional stratigraphy non-conformably overlies a Variscan basement and comprises Permian to Middle Triassic continental to shallow-marine successions, locally intercalated with volcanic rocks, overlain by Upper Triassic platform carbonates and Jurassic-Cretaceous pelagic deposits (Bertotti et al., 1993; Cassano, 1986; Schumacher et al., 1997).

Extensional tectonics controlled the Triassic to Jurassic stratigraphy and started at least during the Middle Triassic, as indicated by thickness variations in Anisian and upper Ladinian formations (Fantoni & Franciosi, 2010; Schumacher et al., 1997). Extension reached its maximum rate between the late Norian and Early Jurassic, with a short-lived pause during the late Rhaetian (Bertotti et al., 1993; Bosellini, 1973; Schumacher et al., 1997), and was accommodated by major N-S striking normal faults. These faults shaped the Lombardian Basin—a regional-scale pelagic basin characterized by several intra-basinal structural highs and intervening lows (Berra & Carminati, 2010; Berra et al., 2009; Bertotti et al., 1993) (Figure 1b). Within this framework, the Gaggiano High developed as the uplifted footwall of a major east-dipping normal fault system separating it from the adjacent Lacchiarella Basin depocenter (Figure 1c; Fantoni et al., 2004).

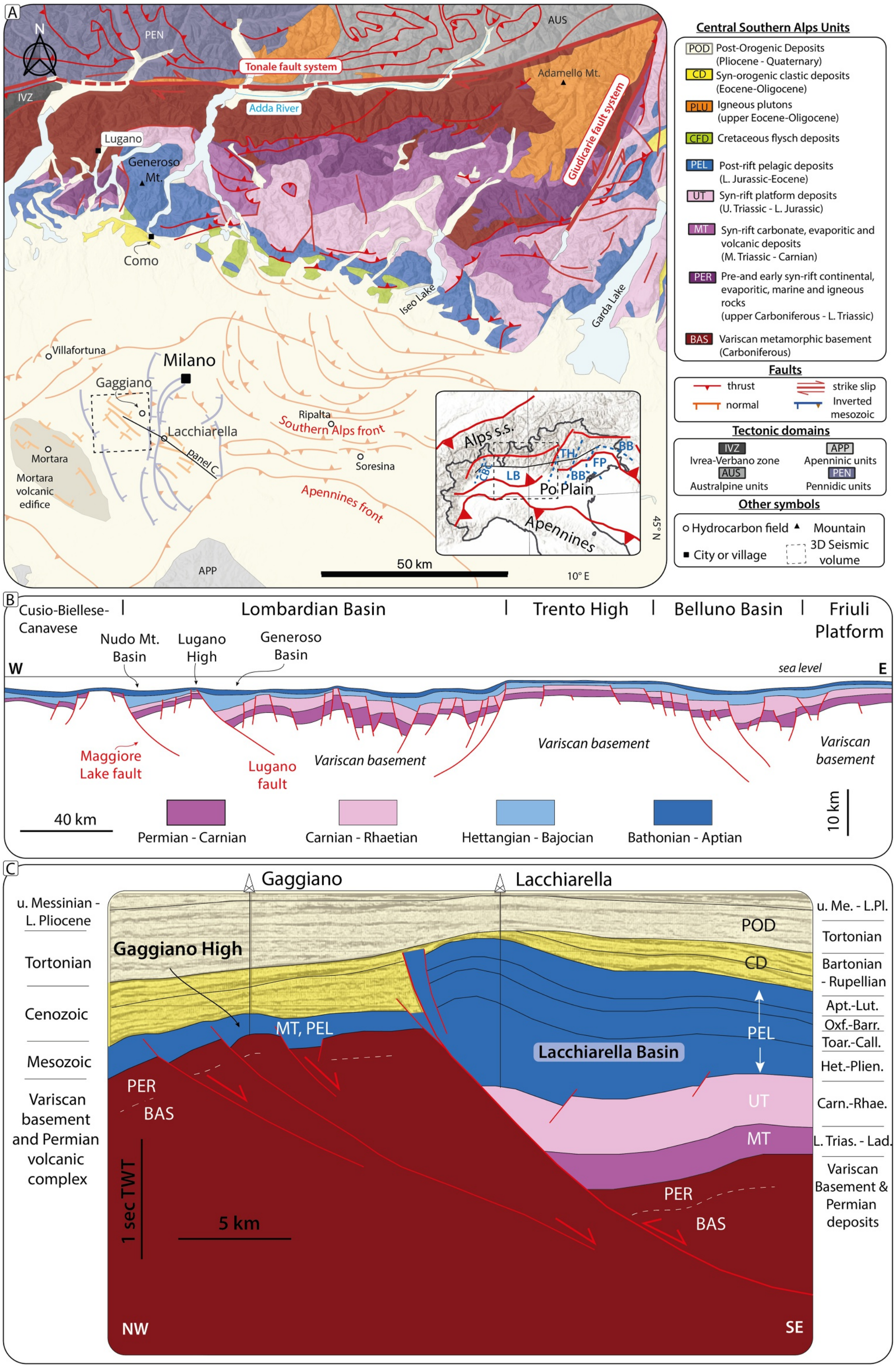

Figure 1. Geological setting of the study area. (a) Simplified geological map of the area shown in the bottom right inset, comprising the Central Southern Alps (CSA) and Western Po Plain (modified from Bigi et al., 1989). The map highlights buried structures beneath the Neogene-Quaternary sediments of the Po Plain, hydrocarbon exploration wells (modified from Fantoni et al., 2004), and tectonic domains. Mesozoic paleogeography is reported with blue letters and dashed lines in the inset. CBC: Cusio-Biellese-Canavese domain; LB: Lombardian basin; TH: Trento High; BB: Belluno Basin; FP: Friuli Platform. (b) Extensional Mesozoic architecture of the Southern Alps at the end of Early Cretaceous (modified after Berra & Carminati, 2010). The trace of the cross-section is shown in the inset of panel (a). (c) Interpreted seismic section across the Gaggiano structure, highlighting the contrast between the Gaggiano High and the Lacchiarella Basin, along with key stratigraphic units and fault systems. The thicker sequence in the hanging wall of the steep W-verging thrust defines this feature as an inversion structure (modified from Fantoni et al., 2004).

West of the Lombardian Basin, the Cusio-Biellese-Canavese sector marks the transition toward the more distal domains of the Adria rifted margin, in the direction of the Ligurian-Piedmontese oceanic domain. This sector records a Triassic-Jurassic stratigraphy that is characterized by abrupt thickness variations, stratigraphic gaps, and unconformities related to the severe rift-related faulting and development of fault-controlled highs and lows along the western Southalpine margin (Berra et al., 2009; Bertotti et al., 1993). In this sector, Jurassic deposits locally rest unconformably on karstified Middle Triassic platform carbonates, documenting prolonged exposure and/or non-deposition before the onset of Jurassic sedimentation (Beltrando et al., 2015).

These characteristics of the Cusio-Biellese-Canavese are consistent with a regional migration of rifting. Extension in the Lombardian Basin continued through the Early Jurassic before shifting westward to the Ligurian-Piedmontese domain in Toarcian time (Berra & Carminati, 2010; Berra et al., 2009; Ferrando et al., 2004), where oceanic spreading started in the Bajocian (Bill et al., 2001). Post-rift thermal subsidence, driven by a reduction in heat flow, led to the accumulation of over 5 km of sedimentary succession in the depocentres and up to ~2 km on intra-basinal highs and plateau (Carminati et al., 2010; Fantoni & Franciosi, 2010; Fantoni & Scotti, 2003) (Figure 1b).

Consistent with this regional pattern, well data from Gaggiano-1 (Bongiorni, 1987) document a condensed stratigraphic record, with a shallow-marine Middle Triassic succession directly overlain by thin Jurassic pelagic limestones and significant gaps spanning the Late Triassic and a large part of the Jurassic. These features indicate persistent structural uplift and long-term non-deposition or erosion on the crest of the high, while coeval thick carbonate successions accumulated in the adjacent Lacchiarella basin (Bongiorni, 1987; Fantoni et al., 2004).

2.3. Cenozoic Inversion and Burial (Cretaceous-Neogene)

Convergence between Adria and Eurasia progressively triggered Alpine-related compressional tectonics, which began in the Late Cretaceous ("eoalpine" phase, e.g., Carminati et al., 1997; Zanchetta et al., 2012) and, during the Cenozoic, induced flexural subsidence with accumulation of pelagic to hemipelagic sediments in the Western Po Plain (Cassano, 1986; Fantoni & Franciosi, 2010). Gentle tectonic inversions in the Villafortuna area are attributed to this same phase (Fantoni et al., 2004).

During the Paleogene ("mesoalpine phase"), NW–SE–striking normal faults developed within the Western Po Plain, locally controlling syn-sedimentary thickness variations within the Scaglia Fm. (Fantoni & Franciosi, 2010). This extensional phase has been associated with coeval magmatic activity, expressed by the development of volcanic edifices in the Euganei-Lessini and Mortara areas (Figure 1a; Fantoni & Franciosi, 2010; Fantoni et al., 1999), and roughly coeval of the emplacement of the Adamello and Bergell plutons in the Southern Alps (Late Eocene–Early Miocene).

The Central Southern Alps and Po Plain underwent predominant deformation during the late Oligocene–Middle Miocene ("neoalpine phase"), following the Adamello magmatic cycle (Castellarin et al., 1992; Fantoni & Franciosi, 2010; Schönborn, 1992; Schumacher et al., 1997). During this interval, strong Alpine-related inversion of Mesozoic extensional structures occurred (Fantoni et al., 2004). Oligocene to Miocene compression induced pronounced positive inversion and folding in the Lacchiarella Basin, forming the present-day buried anticline, whereas the Gaggiano High was only gently tilted (Figure 1c; Fantoni et al., 2004; Turrini et al., 2016, 2018).

From the late Messinian onward, the deformation front of the Northern Apennines advanced into the southern Po Plain, contributing to foreland–basin development and flexural tilting (Argnani & Lucchi, 2001; Ghielmi et al., 2010). Both Alpine and Apenninic thrust systems are now buried beneath the thick Neogene-Quaternary infill of Po Plain (Cassano, 1986; Fantoni et al., 2004; Ghielmi et al., 2010, 2013; Pieri & Groppi, 1981).

3. Data and Methods

This study is based on the interpretation of a 3D seismic reflection data set covering approximately 14 × 13 km in the Gaggiano area, Western Po Plain (northern Italy). The data set was acquired by Agip (now Eni) in the late 1980s and consists of 578 inlines trending approximately N-S and 419 crosslines oriented E-W (Agip, 1987). Three exploration wells drilled along the crest of the structure (Gaggiano-1, Gaggiano-2, and Gaggiano-4-Dir) provide lithostratigraphic calibration and enable correlation between seismic horizons and stratigraphic units (Bongiorni, 1987; Cairo & Ronchi, 1995; Carcano, 1995).

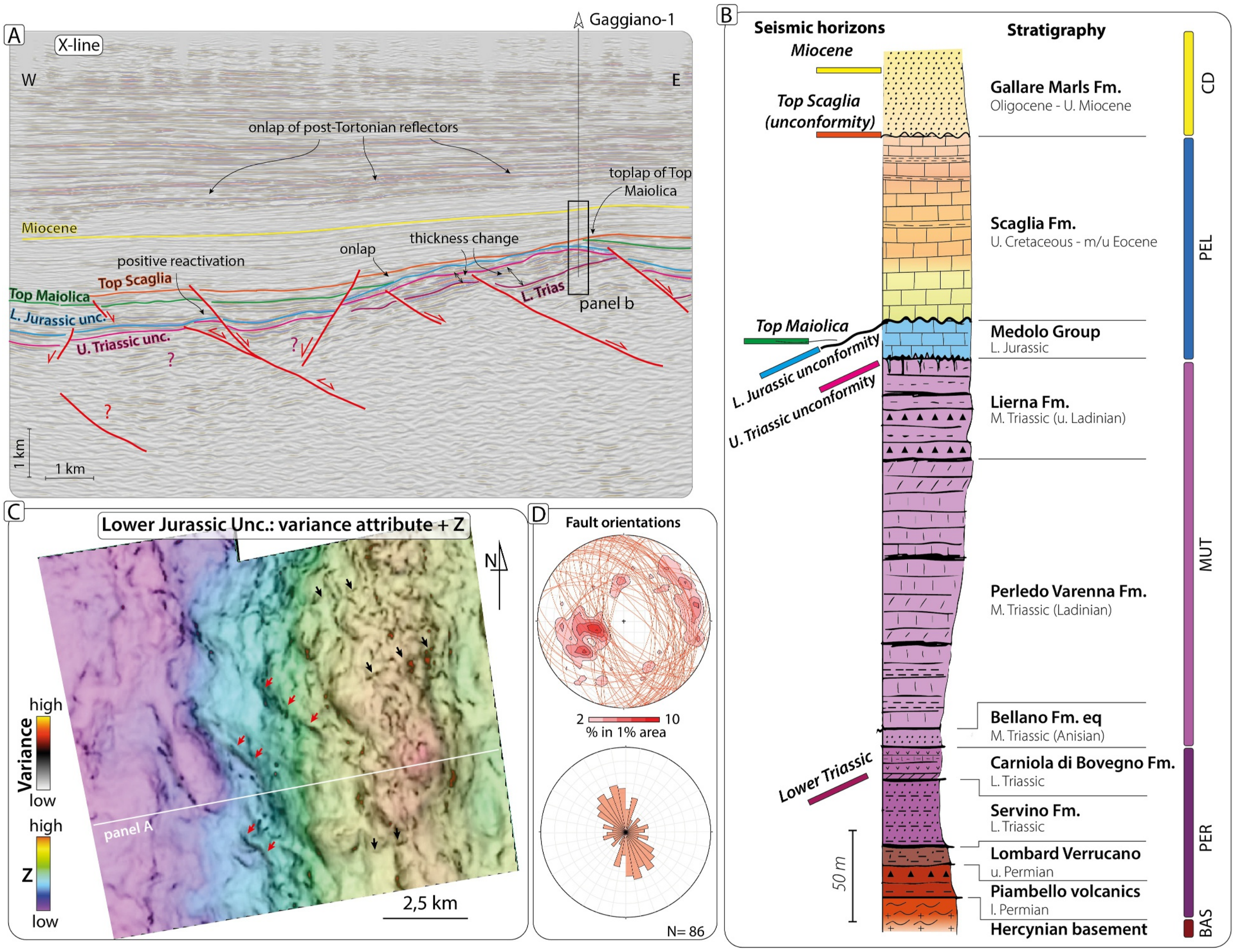

Figure 2. Structural architecture of the Gaggiano High. (a) Interpreted seismic x-line with main fault traces and key horizons; the corresponding uninterpreted seismic line is provided in Figure S1 of Supporting Information S1. (b) Simplified stratigraphic column of the Upper Permian—Miocene interval from the Gaggiano-1 well (see location in panel a). Key stratigraphic horizons interpreted from the 3D seismic volume are indicated on the left. Abbreviations for stratigraphic units (e.g., BAS, PER, MUT) are the same as in Figure 1a. Modified from Bongiorni (1987) and Cairo and Ronchi (1995). (c) Variance attribute map (e.g., Weert et al., 2025) of the Lower Jurassic Unconformity horizon highlighting the fault network. Red and black arrows highlight some of the NW–SE and E–W-striking faults, respectively. (d) Fault orientations represented in equal-area stereonet as a lower hemisphere projection with contour density to poles, and in a rose diagram with 10°-wide petals.

Time-to-depth conversion was performed using a 3D velocity model provided by Eni, derived from well calibration and time-migrated seismic data. The velocity model was implemented in Petrel software and used as the basis for all subsequent structural interpretation.

Six key seismic horizons and 76 faults were interpreted throughout the seismic volume (Figure 2b). To support fault identification and mapping, a variance seismic attribute was also computed and analyzed for selected horizons. Variance highlights lateral discontinuities in seismic reflectors and is commonly used to enhance the imaging of fault surfaces and fault-related features (Chopra & Marfurt, 2007). In this study, variance maps were used qualitatively as an aid to seismic interpretation. From base to top, the interpreted horizons correspond to the Lower Triassic, the Upper Triassic Unconformity, Lower Jurassic Unconformity, Top Maiolica, Top Scaglia, and a Miocene reflector. Horizon selection was guided by both stratigraphic significance and seismic character. The Upper Triassic Unconformity, Lower Jurassic Unconformity, and Top Scaglia represent major discontinuities, whereas the Lower Triassic, Top Maiolica, and Miocene horizons were selected for their strong seismic reflectivity and lateral continuity. Together, these surfaces define the principal tectono-stratigraphic boundaries and record the progressive evolution from Triassic rifting to Neogene contraction.

The Upper Triassic Unconformity coincides with the reflector associated with the absence of the Upper Triassic succession on the crest of the Gaggiano High, as documented by the Gaggiano-1 well (Bongiorni, 1987; Cairo &

Ronchi, 1995). Although this reflector was traditionally mapped in subsurface studies as a Carnian unconformity, the available well correlations indicate that it represents a broader composite hiatus at the top of the Middle Triassic succession, likely resulting from prolonged non-deposition and/or erosion during fault-controlled uplift of the structural high. Comparable stratigraphic condensation, hiatuses and abrupt thickness variations are widely documented along the Triassic-Jurassic rifted margin of the Western Southern Alps, where fault-bounded structural highs and intervening basins controlled sediment preservation during the early evolution of the Alpine Tethys margin (e.g., Berra et al., 2009; Bertotti et al., 1993).

The Lower Jurassic Unconformity lies above the condensed Lower Jurassic deposits of the Medolo Group (Figure 2b). Available well and seismic constraints indicate a broad Lower Jurassic age for this reflector, but do not allow a more precise chronostratigraphic attribution. It is therefore interpreted as a composite surface related to a renewed non-deposition, condensation, and/or erosion on the crest of the Gaggiano High during the Early Jurassic.

Horizon and fault picking was performed at intervals of 10 inlines (~300 m) and 10 crosslines (~250 m). Interpreted horizons were converted into 3D surfaces and integrated with fault polygons within Petrel's structural-modeling environment. All horizons except the Top Maiolica were tied to the three wells, ensuring consistency between seismic interpretation and stratigraphic control. The wells are located along the most elevated portion of the structure, approximately aligned along a N-S trend, with a maximum spacing of ~1.5 km between the northernmost and southernmost wells in map view.

Here, we focus on reconstructing the tectono-stratigraphic evolution and long-term structural preservation of the Gaggiano High through an integrated interpretation of 3D seismic data calibrated by well stratigraphy. This interpretation provides the basis for:

1. The *identification of key stratigraphic surfaces*, including unconformities, and the constraint of the timing of tectonic events.
2. The construction of *structural maps* illustrating the geometry, elevation, and spatial distribution of the main stratigraphic horizons and fault systems.
3. The generation of *isochore (thickness) maps* showing spatial variations in stratigraphic thickness between successive horizons, interpreted as indicators of syn-sedimentary fault activity, erosion, or post-rift subsidence.
4. The analysis of *fault-throw variations along strike and through time*, obtained by sampling vertical throw along fault traces at multiple stratigraphic levels, to assess the relative contribution of Mesozoic and Paleogene extensional phases to the present-day architecture of the Gaggiano High.

The integration of these analyses allows identification of the principal tectonic phases affecting the Gaggiano High, from Triassic extension to Neogene contraction, and supports a reconstruction of the long-term evolution and preservation of this buried structural high within the Western Po Plain.

4. Results

4.1. Structural Architecture

The seismic interpretation reveals a fault system that affects the entire Mesozoic succession (Figure 2a). The dominant structures are N-S-striking, east-dipping faults, accompanied by antithetic west-dipping faults that define a set of west-tilted fault blocks (Figures 2a, 2c, and 2d). The Gaggiano High occupies the footwall of the main east-dipping fault, while the adjacent Lacchiarella area corresponds to a structurally lower domain located east of the studied seismic volume (Figures 1a, 1c, and 2a).

The main N-S fault can be traced through the entire seismic volume, and it displays the largest vertical offset, reaching ~900 m at the Lower Triassic horizon and gradually decreasing upward. Secondary faults are shorter (≤5 km in map view) and show smaller displacements (Figure 2a).

Two subordinate fault sets are present (Figure 2d):

- NW–SE-striking faults (~320°), moderately long (2–5 km), dipping either to the southwest or northeast (Figure 2c).
- E-W-striking faults (~80°), short (≤1 km), mainly confined between the major N–S structures (Figure 2c).

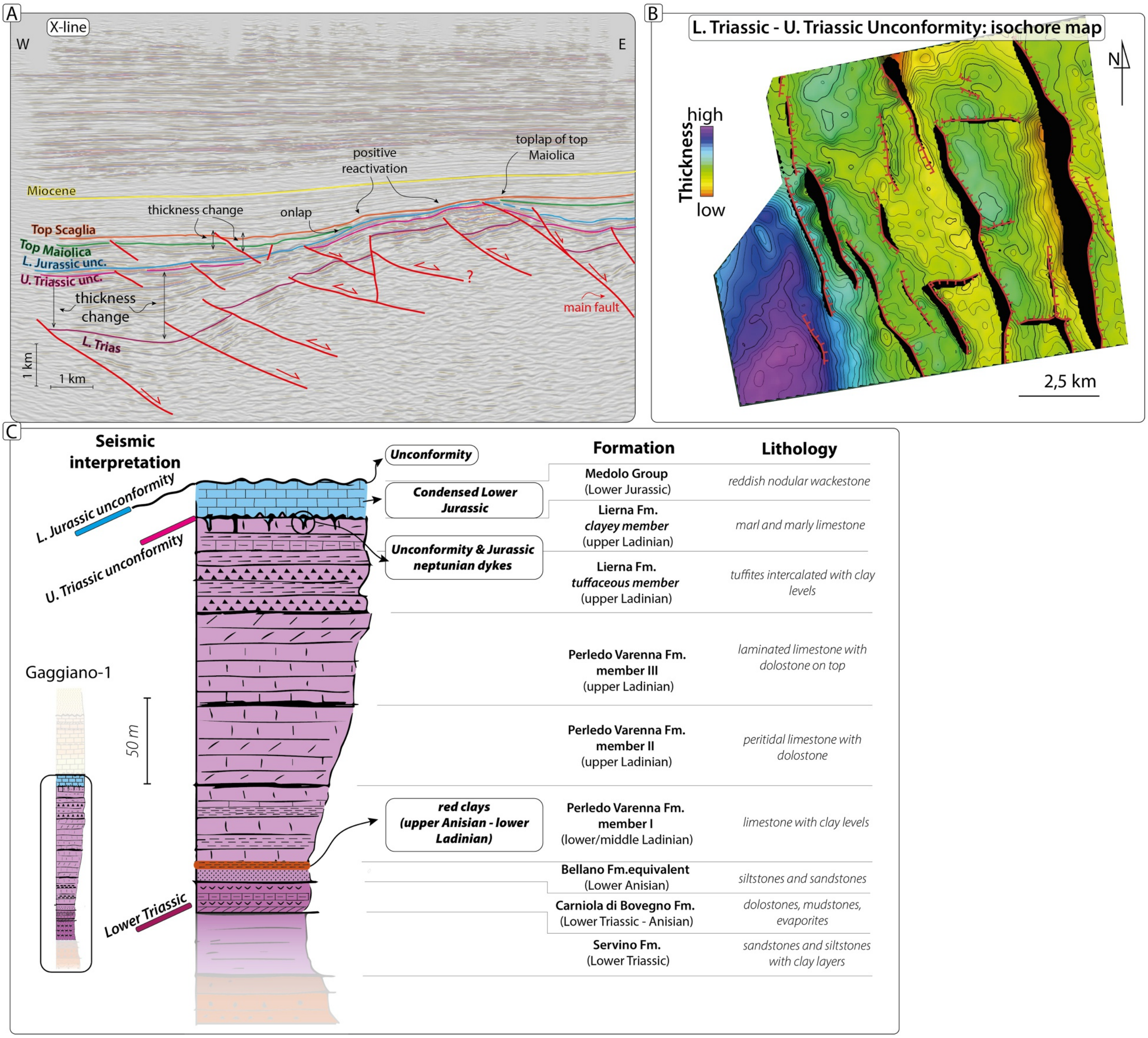

Figure 3. Seismic and well data of the Lower Triassic—Lower Jurassic interval. (a) Interpreted seismic x-line with main fault traces and key horizons; the corresponding uninterpreted seismic line is provided in Figure S2 of Supporting Information S1. (b) Isochore map of the Lower Triassic—Upper Triassic unconformity interval showing thickness variations and tectonic control. Vertical distance between contour lines is 50 m. (c) Stratigraphy of the Lower Triassic—Lower Jurassic interval from the Gaggiano-1 well. Modified from Bongiorni (1987) and Cairo and Ronchi (1995).

In cross-section (i.e., x-lines), the Mesozoic horizons show a consistent westward tilt, whereas the Miocene horizon is continuous and gently dipping, unaffected by faulting (Figure 2a).

4.2. Lower Triassic—Lower Jurassic Interval

Seismic sections and structural maps show that this interval is affected by N–S-striking, east-dipping faults forming a series of west-tilted fault blocks. The main fault, traceable across the entire volume, displays a maximum offset of about 900 m at the Lower Triassic horizon and progressively decreases upward. Minor antithetic west-dipping faults occur in the footwall, whereas NW–SE and E–W faults define shorter segments that connect or terminate against the main structures. The main faults extend upward to the Lower Jurassic Unconformity, which represents the youngest horizon affected by visible offsets (Figures 2a and 3a).

Reflectors between the Lower Triassic and Upper Triassic Unconformity show divergent geometries between fault blocks, and the unconformity truncates underlying reflectors. This surface correspond to the stratigraphic discontinuity marking the absence of the Upper Triassic succession at Gaggiano-1, where shallow-water to intra-platform basin carbonates are overlain by a condensed Lower Jurassic pelagic interval (Figure 3a).

The Lower Jurassic Unconformity forms a smooth, gently upward-convex surface above the condensed Lower Jurassic pelagic interval, marking the transition from the fault-controlled Triassic-Lower Jurassic architecture to the overlying, more continuous reflectors (Figure 3a).

The Gaggiano-1 well documents thin Lower Triassic deposits overlain by terra rossa levels of Anisian-Ladinian age, followed by Middle Triassic shallow-water to intra-platform basin carbonates. The Upper Triassic succession is absent, and the Lower Jurassic interval is condensed, represented by thin nodular red pelagic limestones. This vertical pattern matches the seismic evidence for reduced thickness and reflector discontinuity above the structural crest (Figure 3c).

Structural and isochore maps confirm marked lateral thickness variations within both the Lower Triassic-Upper Triassic Unconformity and Upper Triassic Unconformity-Lower Jurassic Unconformity intervals. Maximum thickness values occur along the hanging-wall domains of the main faults, while the intervals thin markedly above the crest of the Gaggiano High. Depocenters align with the main N-S fault traces, defining an asymmetric pattern with elongated lows in the hanging-wall of N-S faults and minimum values in the footwall blocks (Figure 3b).

4.3. Lower Jurassic Unconformity-Top Maiolica Interval

Seismic sections show that the interval between the Lower Jurassic Unconformity and the Top Maiolica is characterized by continuous reflectors corresponding to pelagic carbonates such as the Maiolica Formation (Figures 2a and 3a). These reflectors display onlap geometries against the Lower Jurassic Unconformity, which forms a gently west-tilted surface in the footwall of the main N-S fault (Figures 2a and 3a). Near this fault, the unconformity shows normal offset and gentle bending, with a local eastward dip related to drag along the fault surface, whereas it gradually recovers a westward inclination moving eastward away from the fault zone (Figures 2a and 3a).

This interval is cross-cut by NW–SE-striking faults, which locally displace the Top Maiolica horizon and produce minor (∼100 m) normal offsets. The interval remains thin and eventually disappears above the crest of the Gaggiano High, then gradually thickens westward, with a more pronounced thickening east of the main N-S fault toward the Lacchiarella area (Figures 2a, 3a, and 4a).

Stratigraphic data from the Gaggiano-1 well indicate the absence of a large part of the stratigraphic record on the crest of the Gaggiano High, where only a thin, condensed pelagic carbonate unit referable to the Lower Jurassic is preserved directly above the Middle Triassic succession (Figure 3c).

4.4. Top Maiolica—Top Scaglia Interval

Seismic sections show that the Top Scaglia surface forms a continuous, gently undulating reflector that blankets the Gaggiano High and smooths the pre-existing relief (Figures 2a and 3a). Reflectors between the Top Maiolica and Top Scaglia horizons are parallel and laterally continuous (Figures 2a and 3a). No major offsets are visible along the main N-S fault, and the overall reflector configuration indicates a uniform geometry across the area (Figures 4a–4c).

Isochore maps of the Top Maiolica-Top Scaglia interval reveal moderate thickness variations associated with NW–SE-striking faults (Figure 4c). These faults locally produce subtle thickening or thinning of the interval and are more frequent than in the underlying units (Figure 4d).

Structural maps confirm that the number of NW–SE faults increases upward, from the Lower Jurassic to the Maiolica and Scaglia horizons, forming short, discontinuous segments that connect or terminate against the main N-S structures (Figures 4a and 4b).

4.5. Top Scaglia-Post-Miocene Interval

Seismic sections show that the interval between the Top Scaglia and the overlying reflectors is characterized by high continuity reflectors which display broad, low-amplitude undulations that are most evident in the hanging wall of the N-S faults (Figures 2a and 3a).

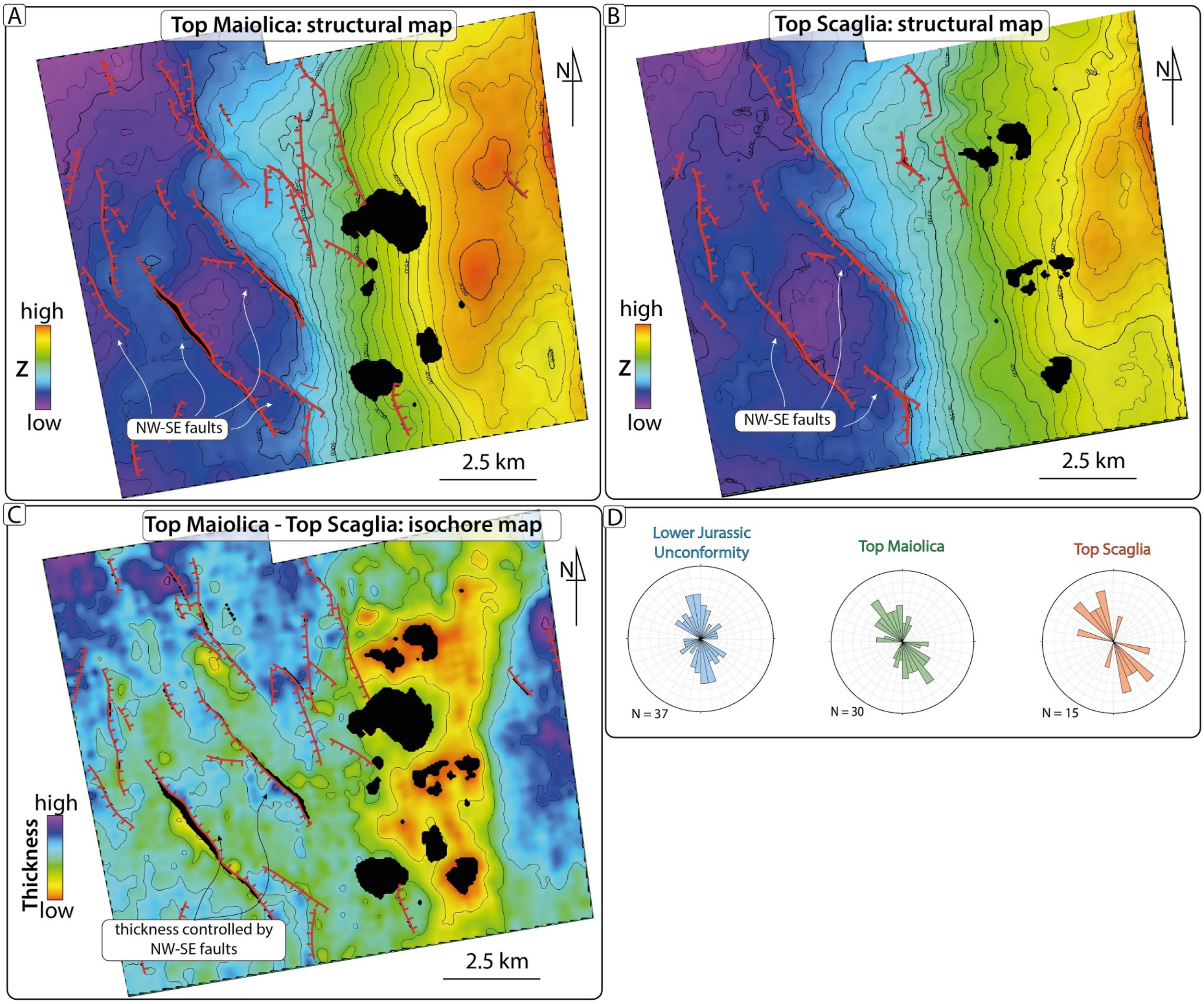

Figure 4. Structural and isochore maps of the Top Maiolica—Top Scaglia interval. (a) Structural map of the Top Maiolica horizon. (b) Structural map of the Top Scaglia horizon. (c) Isochore map of the Top Maiolica—Top Scaglia interval showing thickness variations across NW–SE striking faults. Vertical distance between contour lines is 50 m. (d) Fault orientations across Lower Jurassic Unconformity, Top Maiolica, and Top Scaglia represented in rose diagrams with 10°-wide petals.

Along some cross-lines, the Top Maiolica horizon terminates in toplap against the Top Scaglia surface, which represents a significant discontinuity separating the Cretaceous-Paleogene sequence from the overlying units (Figures 2a and 3a). In the Gaggiano-1 well, this discontinuity corresponds to a distinct unconformity between the pelagic carbonates of the Scaglia Formation and the overlying siliciclastic succession (Figure 2b).

The Miocene horizon, internal to the Neogene succession, forms a continuous, high-amplitude reflector that dips gently southward across the study area (Figure 5a). Above this level, younger reflectors display onlap geometries, particularly toward the south, where sub horizontal post-Tortonian strata lap onto the tilted Miocene succession (Figure 5a). The post-Tortonian deposits show no evidence of internal faulting or deformation at the seismic scale (Figure 5a).

Isochore maps of the Top Scaglia-Miocene interval reveal a progressive thickening toward the north, while the succession above the Miocene thickens to the south (Figures 5a and 5b).

4.6. Throw Versus Distance Diagrams

Maps of fault traces plotted at the deepest and shallowest seismic horizons intercepted by each fault (Figures 6a and 6b) highlight marked differences in fault continuity and vertical persistence across the fault network. In

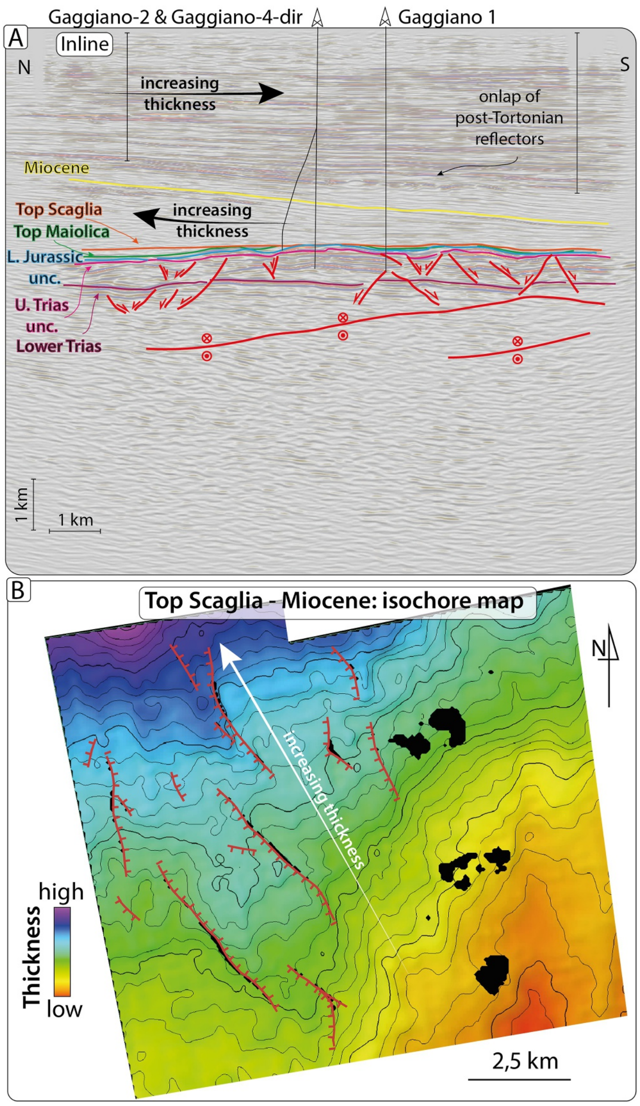

Figure 5. Seismic data from the Top Scaglia—Miocene interval. (a) Interpreted seismic inline with main fault traces and key horizons; the corresponding uninterpreted seismic line is provided in Figure S3 of Supporting Information S1. (b) Isochore map of the Top Scaglia—Miocene interval showing increasing thickness toward the N-NNW. Vertical distance between contour lines is 50 m.

Figure 6a, each fault is represented at the deepest stratigraphic level at which it is observed, revealing that N–S–striking faults form long, laterally continuous structures at depth and dominate the fault pattern, whereas NW–SE–striking faults are fewer and spatially discontinuous.

In Figure 6b, fault traces are shown at the shallowest stratigraphic level displaced by each fault. This representation shows that only a subset of the deep-rooted faults propagates upward to shallower horizons, while several N–S–striking structures terminate at depth and are no longer expressed at higher stratigraphic levels. In contrast, NW–SE–striking faults display a relatively higher persistence at intermediate stratigraphic levels, locally displacing the Top Maiolica and, in some cases, the Top Scaglia horizon. Several faults display curved traces, locally transitioning from N-S to NW–SE orientations along strike (Figure 6b). These depth-dependent variations in fault expression provide a geometric framework for the throw–distance patterns documented in Figures 6c–6f.

Throw-distance diagrams were constructed for four representative faults, including two N-S-striking faults and two NW–SE-striking faults, to quantify along-strike throw variations and compare displacement magnitudes at different stratigraphic levels and for different fault orientation sets (Figure 6). For each fault, throw values were measured at all intercepted seismic horizons, allowing direct comparison between throw associated with early Mesozoic extension (Triassic-Early Jurassic) and younger throw components related to Paleogene tectonics. Early Mesozoic extension is recorded by Lower Triassic, Upper Triassic Unconformity, and Lower Jurassic Unconformity, whereas the Top Maiolica and Top Scaglia horizons record only deformation that postdates the deposition of the Maiolica Fm.

The two N–S striking faults show the greatest along-strike continuity and the highest throw values within the analyzed set, although they differ in maximum displacement (Figures 6c and 6d). The fault shown in Figure 6c exhibits a relatively flat-topped throw profile with values around ∼200 m and local minor peaks, reaching a maximum throw of ∼300 m at the Lower Triassic horizon. Throw decreases upward across the Upper Triassic and Lower Jurassic unconformities and is further reduced at the Top Maiolica horizon. In contrast, the master N-S fault (Figure 6d) displays substantially larger throw, with values at the Lower Triassic horizon approaching ∼800–900 m. Its along-strike throw profile is double-peaked and asymmetric, with two main throw maxima—the highest located in the southern sector—separated by a lower-throw zone. At the Lower Jurassic Unconformity, the throw profile becomes single-peaked, with maximum values around ∼200 m occurring in correspondence with the minimum-throw zone observed at the Lower Triassic horizon. The Top Maiolica and Top Scaglia horizons are not displaced by this fault. Despite these differences, both N-S-striking faults display a systematic decrease in throw toward shallower stratigraphic levels.

NW–SE-striking faults are shorter and characterized by lower throw magnitudes compared to the N-S structures (Figures 6e and 6f). Their throw profiles are irregular and commonly asymmetric, with localized maxima and abrupt along-strike variations. In both analyzed faults, maximum throw values are recorded at the Top Maiolica horizon, reaching ∼180 and ∼130 m for the faults reported in Figures 6e and 6f, respectively. Slightly lower throw values (∼120 m) are observed at the Lower Jurassic Unconformity in both cases. Throw decreases both downward and upward from the Top Maiolica horizon: toward deeper stratigraphic levels, values progressively reduce at the Upper Triassic Unconformity, whereas toward shallower levels a more pronounced decay is observed, with throw at the Top Scaglia horizon limited to a few tens of meters. This vertical distribution defines a non-monotonic throw pattern, with a mid-stratigraphic maximum and reduced displacement at both deeper and shallower levels.

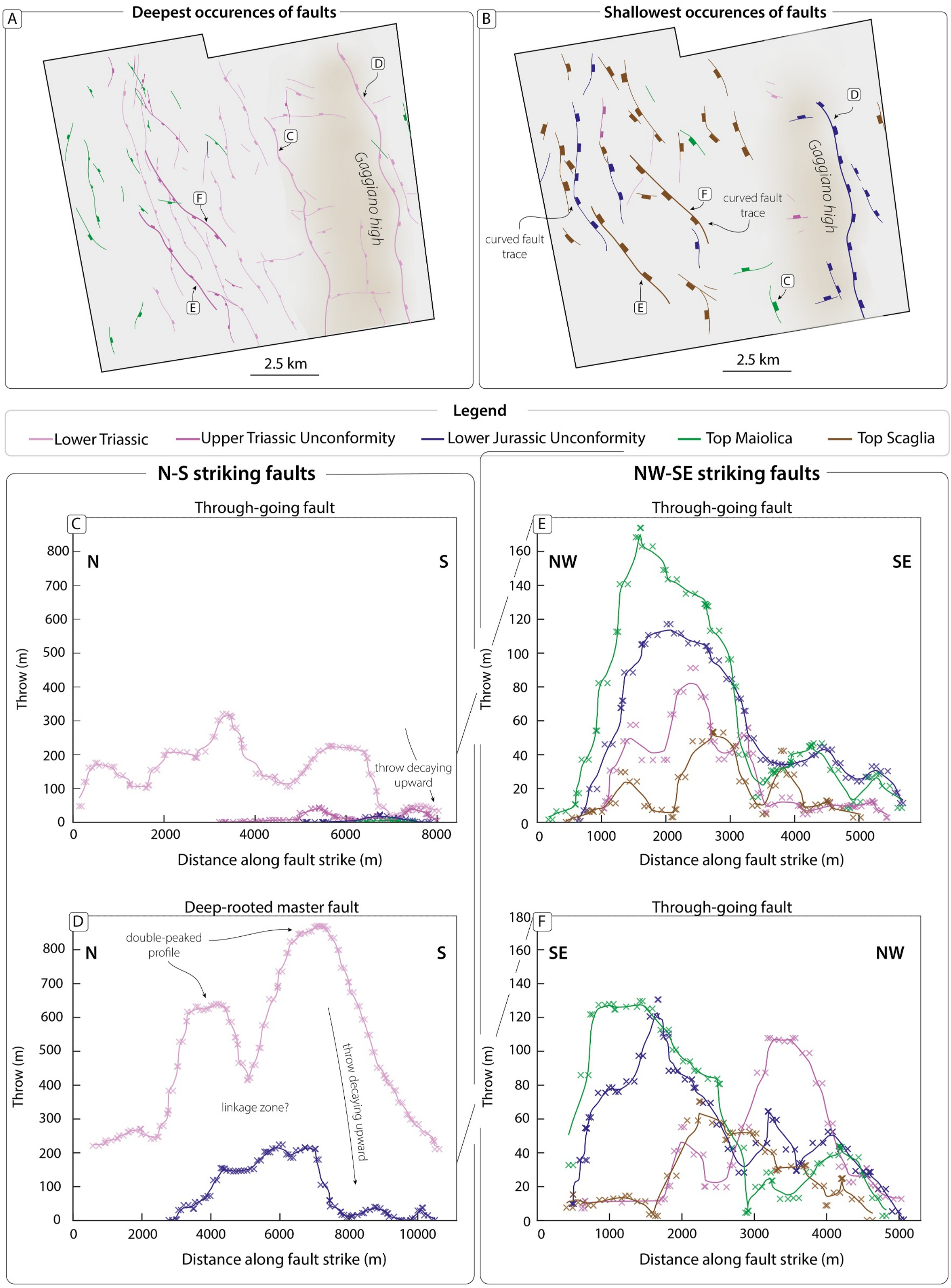

Figure 6. Throw-distance analysis for selected faults within the Gaggiano High. (a, b) Plots showing fault traces in map view at their deepest (a) and shallowest (b) intersections with the interpreted seismic horizons. Fault segments are color-coded according to the stratigraphic horizon displaced by each fault. The shaded brown area highlights the approximate extent of the Gaggiano High. (c–f) Throw-distance diagrams for two N-S-striking faults (c, d) and two NW–SE-striking faults (e, f) highlighted in panels (a) and (b). Throw values (cross symbols) are color-coded according to the displaced seismic horizon. For each fault, throw measurements were projected orthogonally onto a common reference line approximating the mean fault strike. Smoothed throw profiles were obtained by applying a moving-average filter (window size = 5) followed by Piecewise Cubic Hermite Interpolating Polynomial (PCHIP) interpolation.

5. Discussion

5.1. Geological Evolution of the Gaggiano High

The results presented above document the long-term structural and stratigraphic evolution of the Gaggiano High from the Triassic to the present. The 3D seismic interpretation, integrated with well data and isochore maps, reveals a fault-controlled Mesozoic architecture dominated by N-S-striking, east-dipping normal faults, progressively overlain by a smoother and more continuous post-rift succession.

The Lower Triassic-Lower Jurassic interval records the highest degree of deformation, with major thickness variations, reflector divergence, and a strongly condensed stratigraphic record above the crest of the high (Figure 3). The overlying Jurassic-Cretaceous succession is characterized by continuous pelagic reflectors onlapping the Lower Jurassic Unconformity, indicating persistent structural relief during post-rift subsidence (Figures 2a and 3a). In contrast, the Top Maiolica-Top Scaglia interval displays laterally continuous reflectors that blanket the high, accompanied by localized thickness variations associated with NW–SE-striking faults (Figures 2a, 3a, and 4). Finally, the Top Scaglia-Top Miocene interval records gentle folding, regional tilting, and progressive burial beneath the Neogene foreland deposits (Figures 2a, 3a, and 5).

Together, these observations indicate a transition from a strongly fault-controlled Mesozoic extensional framework to a progressively smoother and less faulted Cenozoic architecture, preserving a clear stratigraphic record of the long-term evolution of the Gaggiano High. On this basis, four main tectono-stratigraphic stages can be identified and are discussed below.

5.1.1. Middle to Late Triassic: Domino-Style Extension and Local Exposure

This interval records a phase of domino-style extensional tectonics active since the Anisian–Ladinian (Figures 7a–7c). These patterns support an early phase of extension during the Middle Triassic (Fantoni & Franciosi, 2010; Schumacher et al., 1997).

Well data record a residual red clay horizon capping the Lower Anisian deposits, interpreted as a weathering surface related to subaerial exposure prior to Ladinian sedimentation (Cairo & Ronchi, 1995). The thinned Lower Triassic deposits and terra rossa levels indicate footwall uplift and local subaerial exposure of the high (Figure 7a). Subsequent subsidence is indicated by shallow-water carbonate deposition during the Middle Triassic (Figure 7b). During the Late Triassic-Early Jurassic, a renewed phase of fault-controlled uplift and differential subsidence, constrained by the continuation of fault offsets up to the Lower Jurassic Unconformity, marks the complete structural definition of the Gaggiano High (Figure 7c). During this stage, the crest of the high likely underwent prolonged non-deposition and/or erosion, producing the hiatus recorded by the Upper Triassic Unconformity.

5.1.2. Jurassic to Early Cretaceous: Regional Subsidence and Persistent Structural Relief

Observations from the Lower Jurassic–Top Maiolica interval (Section 4.3)—continuous pelagic reflectors onlapping the Lower Jurassic Unconformity and the condensed Jurassic succession in the well—indicate that, during post-rift thermal subsidence, the Gaggiano High remained topographically elevated (Figure 7d; Bongiorni, 1987; Fantoni et al., 2004).

The persistent thinning of the Jurassic–Cretaceous intervals above the crest and their lateral onlap toward the flanks demonstrate that sediments preferentially accumulated in the adjacent Lacchiarella depocenter, while the high acted as a stable structural relief throughout the Jurassic to Early Cretaceous (Figure 7d).

5.1.3. Middle to Late Eocene: Renewed Extension Along NW–SE Faults

Thickness variations and localized offsets observed in the Top Maiolica–Top Scaglia interval (Section 4.4), together with the increasing number of NW–SE faults in the structural maps, indicate a renewed extensional episode during the middle to late Eocene (Figure 7e).

This deformation was accommodated by NW–SE-striking normal faults, which reach the Top Scaglia horizon but do not affect Miocene strata, constraining their activity to pre-Neogene times. Syn-sedimentary growth across

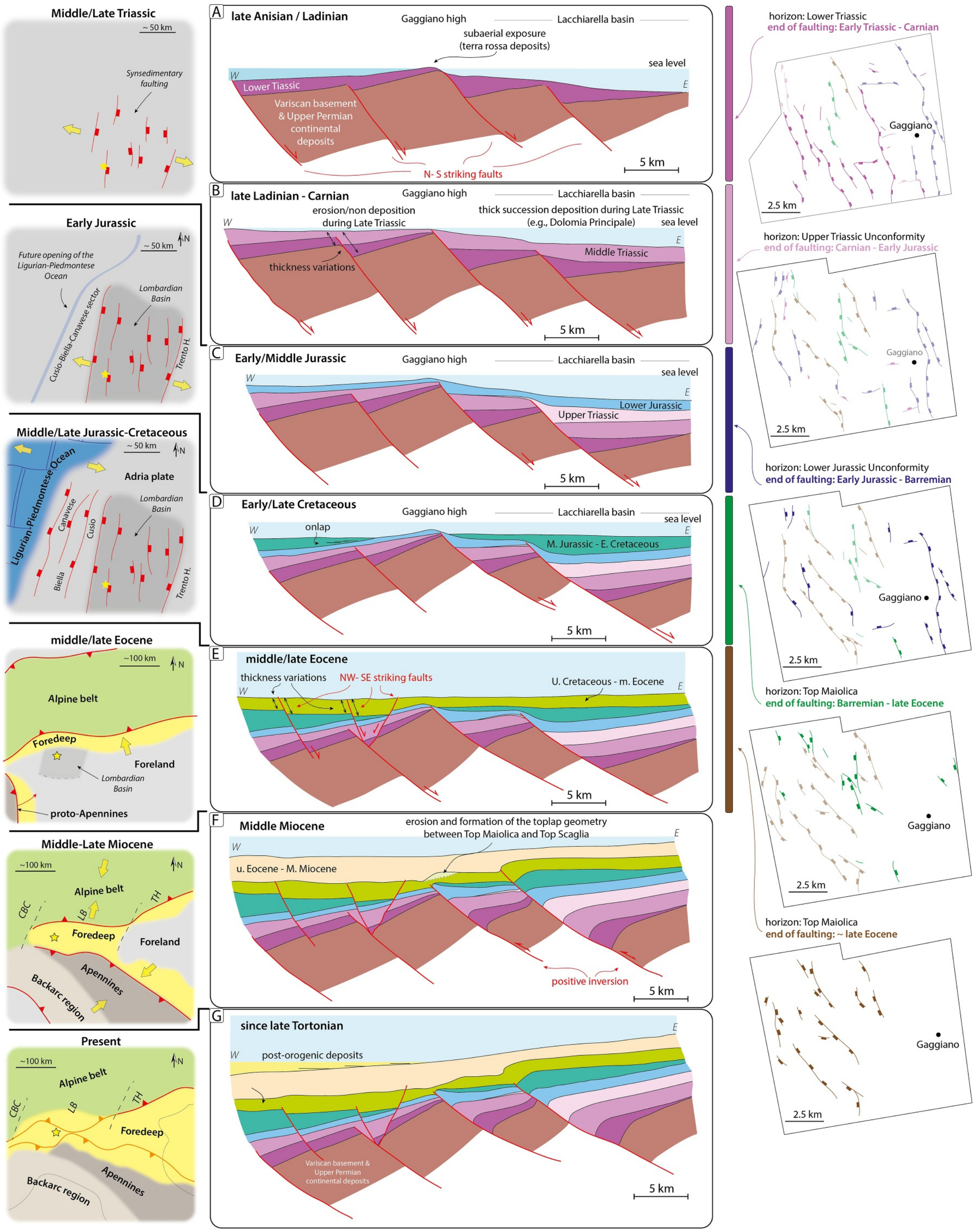

Figure 7. Structural evolution of the Mesozoic Gaggiano High and the adjacent Lacchiarella basin within the regional evolution of the western Adria margin. Left panels show schematic regional tectonic cartoons illustrating the position of Gaggiano from Middle-Late Triassic onset of rifting to present-day burial within the Alpine-Apennine foreland-foredeep system. Cartoons are modified from Berra et al. (2009), Carminati et al. (2012), and Turrini et al. (2016). The yellow star indicates the approximate location of Gaggiano. CBC: Cusio–Biellese–Canavese sector; LB: Lombardian Basin; TH: Trento High. Central panels illustrate the main tectono-stratigraphic stages from late Anisian extension to Oligocene-Miocene inversion and post-orogenic deposition. Note that Mesozoic faults were progressively rotated, and their present-day shallow dip results from this rotation. Maps to the right show fault traces at selected stratigraphic horizons, color-coded according to the shallowest occurrence (i.e., the youngest horizon intersected by each fault). For each map, only faults whose shallowest occurrence corresponds to the displayed horizon are shown with full opacity, whereas faults extending to shallower levels are displayed transparently. *The scales for the left and central panels are approximate and for illustrative purposes only.*

these faults, expressed by local thickening of the Scaglia interval, suggests that part of the deformation occurred during deposition of the Scaglia Formation (Figure 7e).

Several NW–SE faults merge downward with the main N–S fault system, defining a composite fault architecture that likely reflects reactivation of inherited Mesozoic faults under a modified stress regime (Figures 2a, 4a, 4b, and 7e).

Locally, some seismic profiles show minor folds in the hanging wall of the N–S faults, probably caused by positive inversion or buttressing, which are cross-cut by NW–SE faults. This geometry may indicate a limited contractional phase predating the extensional faulting along the NW–SE faults (Figure 2a).

5.1.4. Oligocene to Late Miocene: Contraction, Folding, and Final Tilting

The gentle folding of pre-Miocene horizons and the unconformity at the Top Scaglia surface indicate a phase of far-field contraction during the Oligocene–Miocene, likely associated with the advancing Western Southern Alps front. This deformation led to partial positive (transpressional) inversion of pre-existing N–S faults and localized erosion at the crest (Figure 7f).

Isochore maps of the Top Scaglia–Miocene interval show northward thickening of the Oligo–Miocene succession (Figure 5), consistent with flexural subsidence in the northern sector related to the development of the Southern Alps (Bertotti et al., 1998).

The southward dip of Miocene reflectors and the onlap of post-Tortonian strata onto the tilted Miocene surface mark a subsequent southward tilting of the area, attributed to flexuring of the foreland under the advancing Northern Apennines (Figures 5 and 7g; Cassano, 1986; Fantoni & Franciosi, 2010). The end of tectonic activity at the seismic scale is constrained by sub-horizontal Messinian reflectors, which seal the tilted succession and mark the transition to structural quiescence and burial beneath the Po Plain deposits (Figures 2a, 5a, and 7f).

5.2. Relative Contribution of Early Mesozoic and Paleogene Fault Activity

Throw-distance analysis provides quantitative constraints on the relative contribution of different tectonic phases to fault growth and displacement accumulation within the Gaggiano High (Figure 6). By comparing throw values measured at lower Mesozoic horizons (Lower Triassic, Upper Triassic Unconformity, and Lower Jurassic Unconformity) with those recorded at higher stratigraphic levels (Top Maiolica and Top Scaglia), it is possible to discriminate between displacement accrued during Triassic-Early Jurassic rifting and younger Paleogene extension.

N–S-striking faults are characterized by large cumulative throw at lower Mesozoic levels, reaching several hundreds of meters and, in the case of the master fault, approaching ~900 m (Figures 6c and 6d). Throw systematically decreases upward and becomes minor or negligible at post-Jurassic horizons, indicating that the dominant displacement along these structures was accommodated during early Mesozoic extension. The absence of displacement at the Top Maiolica and Top Scaglia horizons along the master N–S fault, together with its limited upward persistence documented in the fault-trace maps (Figures 6a and 6b), further supports the limited role of Paleogene reactivation along the main fault system.

In contrast, NW–SE-striking faults display lower cumulative throw and a different vertical distribution of displacement (Figures 6e and 6f), with maximum throw values recorded at the Top Maiolica horizon, whereas throw decreases both downward, toward the Upper Triassic and Lower Jurassic unconformities, and upward, toward theTop Scaglia. This non-monotonic throw pattern indicates that NW–SE faults accommodated only limited displacement during early Mesozoic rifting and were preferentially active during post-Jurassic deformation. Thickness variations across NW–SE faults within the Top Maiolica-Top Scaglia interval and displacement of the Top Scaglia horizon further constrain their main activity to the Upper Cretaceous–Paleogene, with deformation persisting until at least the late Eocene.

The occurrence of curved fault traces at shallow stratigraphic levels, locally transitioning from N–S to NW–SE orientations (Figure 6b), suggests a progressive reorganization of the extensional fault network through time. This geometry is consistent with partial reactivation of inherited N–S–striking faults under a changing stress field, followed by the preferential development of newly oriented NW–SE normal faults once the pre-existing structures became unfavorably oriented. Similar behavior has been documented in polyphase extensional systems,

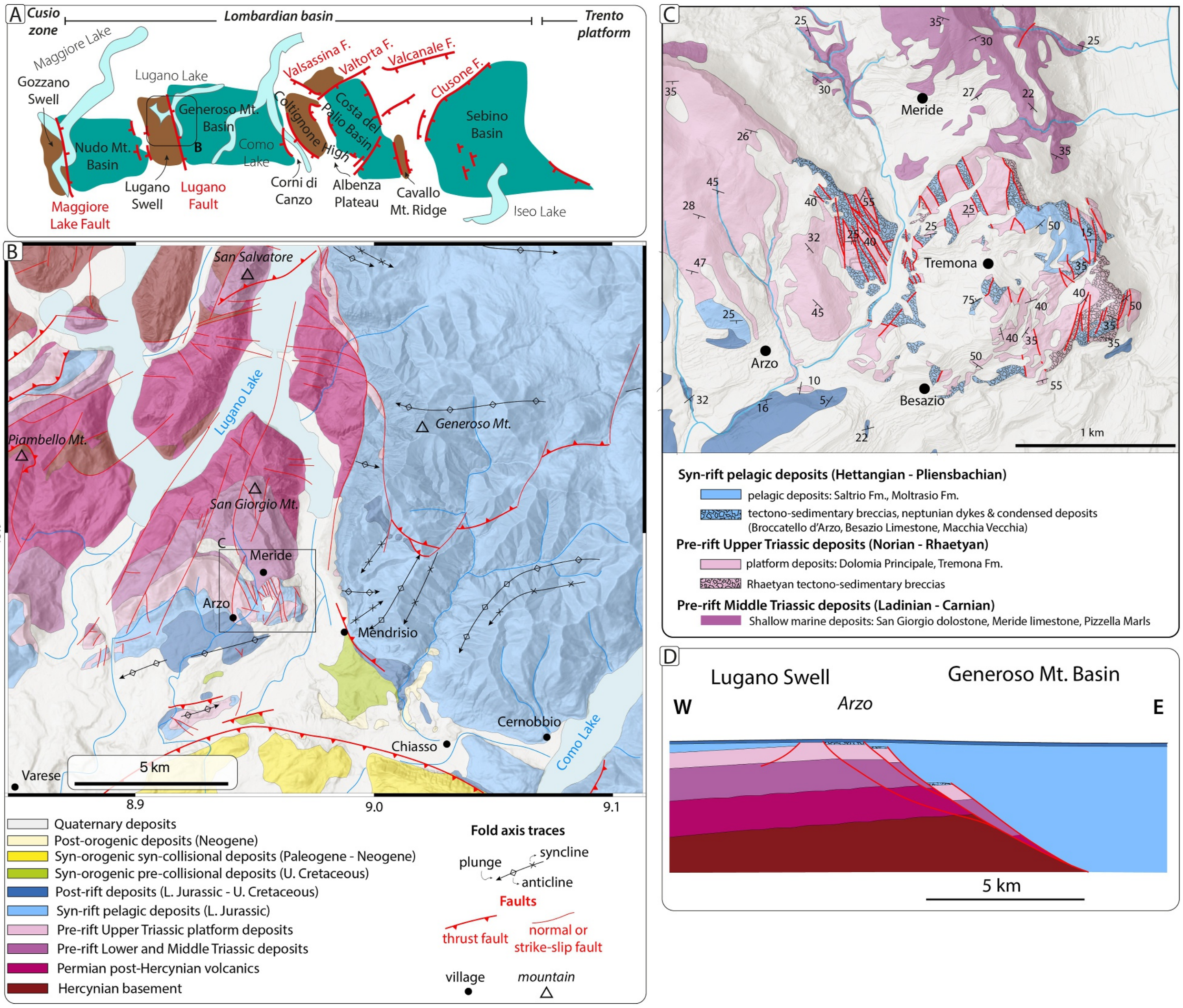

Figure 8. Exhumed analogue for the Gaggiano structural high. (a) Simplified paleogeographic reconstruction of the central Southalpine domain during the Early Jurassic, showing the eastern portion of the Lombardian Basin. The area was characterized by a series of structural highs and lows bounded by N–S- and subordinately E–W-striking extensional faults. (b) Simplified geological map of the Lugano Lake area (see location in panel a), where the tectono-stratigraphic architecture is controlled by Late Triassic to Early Jurassic extensional tectonics (modified after Antognini & Bronzini, 2018). (c) Enlargement of the area indicated in panel (b), showing Rhaetian and Early Jurassic syn-tectonic breccias bounded by N–S-trending normal faults. (d) Palinspastic cross-section illustrating the Lugano Swell during the Middle Jurassic. The structure corresponds to a tilted Late Triassic to Early Jurassic structural high bounded to the east by the Lugano Fault. Hettangian–Sinemurian syn-tectonic breccias are preserved at the crest of the high (modified after Bernoulli et al., 2017).

where stress rotation promotes selective fault reactivation and the nucleation of new fault sets oblique to earlier fabrics (e.g., Bellahsen & Daniel, 2005; Holdsworth et al., 1997; Morley, 2017).

Overall, the throw-distance analysis indicates that the present-day architecture of the Gaggiano High is primarily inherited from Triassic-Early Jurassic extensional tectonics, whereas Paleogene deformation is limited to minor faults and localized reactivation. This quantitative evidence supports the interpretation of the Gaggiano High as a long-lived structural high that largely preserved its early Mesozoic extensional framework through subsequent tectonic phases.

5.3. The Lugano Swell as an Exhumed Analogue for the Gaggiano Structural High

The Lugano Swell, exposed in the central Southern Alps (Figure 8a), provides a valuable analogue for the buried Gaggiano High, as both structures record the long-term evolution of intra-basinal highs developed along the Adria passive margin during Mesozoic rifting. Despite differences in their degree of exposure, stratigraphic preservation, and subsequent involvement in the Neogene contraction, their overall tilted-block geometry and fault architecture display remarkable similarities.

As discussed in Section 5.1, the Gaggiano High originated as a N-S oriented footwall block bounded by east-dipping normal faults and shaped by domino-style extension during Triassic-Jurassic rifting (Figures 7a–7c). Well and seismic data show the complete absence of Upper Triassic deposits and a condensed Lower Jurassic succession resting unconformably on Middle Triassic carbonates, reflecting persistent structural uplift (Figure 3; Bongiorni, 1987; Cairo & Ronchi, 1995). During the Jurassic, pelagic sediments onlapped the structural flanks, while the adjacent Lacchiarella Basin accumulated a thicker coeval succession, defining a strongly asymmetric rift-related architecture (Figures 1c, 2a, and 3a).

A comparable structural setting characterizes the Lugano Swell (Figures 8b–8d), where N-S-striking normal faults developed during the Late Triassic-Early Jurassic extension and controlled the formation of a west-tilted footwall block (Figure 8d; Bernoulli et al., 2017; Bertotti, 1991 and references therein). Syn-tectonic breccias of Rhaetian-Sinemurian age and neptunian dykes document syn-rift deformation (Figure 8c), and the Jurassic succession displays a wedge-shaped geometry thickening toward the W and to the hanging wall basin (Figures 8b–8d), closely resembling the pattern observed in the Gaggiano-Lacchiarella system (Figures 1c and 8d).

The similarity between the Gaggiano High and the Lugano Swell should therefore be considered primarily structural rather than strictly stratigraphic. Both structures record the development of fault-bounded, tilted highs during Triassic-Jurassic extension. However, they differ in the preservation of the Upper Triassic succession. The Lugano Swell retains a thick Upper Triassic succession (Dolomia Principale, ~500 m thick; Figures 8c and 8d), whereas the Gaggiano High records an Upper Triassic hiatus and a strongly condensed Lower Jurassic succession (Bernoulli et al., 2017; Bertotti, 1991; Bongiorni, 1987; Cairo & Ronchi, 1995). In this respect, the Gaggiano High shares closer stratigraphic similarities with the Cusio-Biellese-Canavese sector of the western Southern Alps, where Jurassic deposits locally overlie Middle Triassic platform carbonates across major unconformities and the Triassic-Jurassic succession is characterized by strong thickness variations, condensed intervals, and stratigraphic gaps (Beltrando et al., 2015; Berra et al., 2009; Bertotti et al., 1993).

The Gaggiano High and Lugano Swell highlight the long-term influence of Jurassic rift-related structural inheritance on subsequent Alpine and Apennine deformation. Similar inherited extensional fabrics are known to localize foreland folding and influence thrust propagation in several sectors of the Southern Alps, including the Dolomites (Doglioni, 1992a, 1992b), the Trento Platform and Giudicarie fault system (Castellarin et al., 2006; Prosser, 1998), and the Central Southern Alps (Rocca et al., 2024, 2026; Schönborn, 1992; Zanchi et al., 2012). Recent studies from the Western Southern Alps further demonstrate that rift-related structural highs and inherited normal faults may act as mechanically rigid domains during subsequent contraction, promoting buttressing, back-folding and local deflection or arrest of thrust propagation, rather than simple fault inversion (e.g., Scaramuzzo et al., 2022). In this framework, the largely preserved architecture of the Gaggiano High provides a valuable subsurface reference for interpreting the mechanical role of inherited rift-related highs during later contractional phases, complementing insights derived from exhumed analogs such as the Lugano Swell.

5.4. Tectonic Implications and Regional Significance

The persistence of the Gaggiano High through multiple tectonic cycles illustrates the mechanical strength and rheological contrast between structural highs and intervening basins along the Adria margin. The limited reactivation of the Gaggiano faults during Neogene shortening, compared with the strong inversion recorded in the adjacent Lacchiarella structure (Figures 1c and 6), suggests that the high acted as a mechanical buttress during the propagation of compressional deformation from both the Southern Alps and Northern Apennines (e.g., Butler et al., 2006). Such behavior is consistent with analogue models showing that rift-related fault blocks may localize or deflect compressional strain depending on their relative stiffness and burial depth (Bonini et al., 2012; Sieberer et al., 2023).

This mechanical behavior is likely related to the inherited position of the Gaggiano High within the western Adria rifted margin. The western Southern Alps record the transition from the Lombardian Basin and its intrabasinal highs toward the more distal domains of the Adria margin, represented by the Cusio-Biellese-Canavese sector and, farther west, by the Ligurian-Piedmontese oceanic domain (Beltrando et al., 2015; Berra et al., 2009; Bertotti et al., 1993; Decarlis et al., 2017). Although the available 3D seismic data do not image the full crustal section, the stratigraphic architecture, including the Upper Triassic hiatus and condensed Lower Jurassic succession, suggests that the Gaggiano High belonged to a relatively uplifted and mechanically competent continental domain located close to the proximal-to-distal transition of Adria passive margin. In this framework, the Gaggiano High was not merely a local structural high, but part of an inherited continental block whose position and architecture may have influenced the pathways through which Alpine–Apennine deformation was later transferred, partitioned, or locally inhibited.

The contrasting evolution of the Gaggiano High and Lacchiarella Basin provides a local expression of this inherited mechanical segmentation. The strong inversion affecting the Lacchiarella structure may not represent a pure positive inversion, but rather a transpressional reactivation of the pre-existing extensional fault system. Considering the NNE–SSW-oriented Alpine compression (Castellarin et al., 1992) and the N–S to NNW–SSE strike with eastward dip of the Gaggiano–Lacchiarella fault system, these faults likely acted as oblique ramps accommodating lateral transfer within the Alpine thrust system. By contrast, the Gaggiano High remained comparatively less deformed, preserving much of its Mesozoic extensional architecture.

At the regional scale, the orientation of the Gaggiano fault system is consistent with the main Mesozoic extensional fabric of the Southalpine domain, which controlled the development of intra-basinal highs such as the Lugano Swell, Canzo High, Gozzano Swell and Coltignone High (Bertotti et al., 1993; Castellarin et al., 1992; Winterer & Bosellini, 1981). This inherited architecture exerted a first-order control on the segmentation of the Alpine and Apennine thrust fronts. Neogene contractional structures are preferentially localized above or adjacent to pre-existing Mesozoic basins, whereas areas corresponding to Mesozoic highs show reduced shortening and limited inversion, as documented in Gaggiano (Fantoni & Franciosi, 2010; Livani et al., 2018; Scisciani, 2009; Turrini et al., 2014). This interpretation is consistent with the local recession of the Northern Apennines thrust front in correspondence with the Gaggiano High (see Figure 1a), which may reflect the presence of a mechanically stronger inherited structural domain.

The superposition of two opposite-verging orogenic systems—the Southern Alps to the north and the Northern Apennines to the south—produced a complex pattern of flexural subsidence and gentle tilting during the Neogene (Carminati & Doglioni, 2012 and references therein). The northward thickening of the Oligo-Miocene deposits and the southward tilt of the Miocene reflectors, accompanied by the onlap of post-Tortonian strata (Figures 2a and 5), record the dual influence of the Alpine and Apennine loads, which progressively buried the Gaggiano High without fully reactivating its extensional fault framework. This geometry defines a transitional sector of the Po Plain, located between the opposite deformation fronts of the Southern Alps and Northern Apennines. In this area, the two orogenic systems are structurally independent but flexurally interacting, producing overlapping subsidence and tilting without direct structural linkage (Fantoni & Franciosi, 2010; Turrini et al., 2016).

In addition to the dominant Mesozoic rift inheritance and subsequent Neogene contraction, the structural evolution of the Gaggiano area was also influenced by a Paleogene extensional phase documented at the scale of the Southern Alps and the Adria domain. Several studies have shown that during Cretaceous-Paleogene time Adria experienced a diffuse extensional stress field, locally associated with anorogenic magmatism and characterized by the development or selective reactivation of high-angle normal faults, commonly oriented NW–SE to NNW–SSE (Barbieri & Grandesso, 2007; Fantoni et al., 1999; Vitale & Ciarcia, 2022; Vitale et al., 2018; Zampieri, 1995). At Gaggiano, this extensional phase is recorded by thickness variations within the Upper Cretaceous–Paleogene succession between the Top Maiolica and Top Scaglia horizons (Figures 3a and 4c), which are locally controlled by NW–SE-striking faults. This evidence indicates syn-sedimentary activity during pelagic sedimentation, consistent with a low-magnitude extensional regime superimposed on the inherited Mesozoic structural framework. However, the absence of well-developed Paleogene depocenters and the limited throw of these structures suggest that Paleogene extension did not significantly modify the Jurassic rift architecture but rather resulted in localized reactivation and subtle modulation of sedimentary thicknesses. This interpretation is consistent with regional models that describe Paleogene extension in the Southern Alps and adjacent Adria domain as a phase of renewed extensional tectonics, variably interpreted as a diffuse lithospheric reorganization or as an abortive rifting episode, locally associated with anorogenic magmatism and controlled by inherited structural heterogeneities (Fantoni et al., 1999; Vitale & Ciarcia, 2022; Vitale et al., 2018). In this framework, the Gaggiano High preserves the cumulative imprint of multiple tectonic stages, in which Paleogene extension represents a secondary but detectable overprint on a long-lived rift-related structural high.

6. Conclusions

The Gaggiano High preserves the original geometry of a Mesozoic structural high formed along a N–S extensional fault system and only mildly overprinted by Alpine–Apennine contraction. Its 3D seismic architecture reveals a prolonged structural relief from at least the Middle Triassic to the Early Cretaceous, followed by localized Paleogene reactivation and final burial during the Neogene.

Despite its position within the foreland–foredeep system of the Southern Alps and Northern Apennines, the Gaggiano High retained a well-defined extensional signature, in contrast with adjacent structures such as the Lacchiarella Basin that experienced significant positive inversion. This contrast emphasizes the long-term mechanical influence of inherited rift structures in governing both syn- and post-rift deformation along the western Adria margin.

The Gaggiano High thus represents a rare example of a well-preserved Mesozoic structural high in the subsurface of the Po Plain, providing valuable insights into the persistence, reactivation, and mechanical behavior of inherited fault systems. In particular, it provides a well-constrained subsurface reference to assess how inherited rift-related highs modulate strain partitioning and the spatial distribution of deformation in buried foreland settings.

Conflict of Interest

The authors declare no conflicts of interest relevant to this study.

Availability Statement

The 3D seismic and well data used in this study are proprietary to Eni S.p.A. and were used under a research agreement with Sapienza University of Rome within the framework of the PON-REACT-EU program. Due to confidentiality restrictions, the raw seismic data cannot be shared publicly. Well data are available at https://unmig.mase.gov.it/regolamento-ue-2024-1735-articolo-21-comma-1-lettera-b/. Derived products such as structural maps, interpreted horizons, and thickness maps that do not disclose the original data are available from the corresponding author upon reasonable request, subject to the terms of the data-sharing agreement. 3D seismic interpretation and fault surface modelling were carried out using Petrel™ E&P Software Platform (version 2020.1) by Schlumberger (https://www.software.slb.com/products/petrel). Structural maps, and thickness maps were edited with QGIS (version 3.40.5 "Bratislava"; https://qgis.org/). Figures were produced with Matplotlib version 3.7.1 (Hunter, 2007). Additional visualisation and statistical analyses were carried out with Seaborn version 0.12.2 (Waskom, 2021), Pandas version 1.5.3 (McKinney, 2010), NumPy version 1.24.2 (Harris et al., 2020), and Statsmodels version 0.13.5 (Seabold & Perktold, 2010). All code was run in a reproducible Python environment and is available upon request. Final figure composition and layout were performed using Adobe Illustrator (version 28.0; https://www.adobe.com/products/illustrator.html).

Acknowledgments

This work forms part of a joint project between Sapienza University of Rome and Eni within the framework of the PON-REACT-EU program. It received funding from Sapienza University of Rome through the 2021 "Progetti di Ricerca Medi" program (M. Mercuri) and the 2023 "Progetti di Ricerca Grandi" program (E. Carminati) (Ateneo 2021, Ateneo 2023). The authors wish to thank Dr. Roberto Longoni for stimulating discussions on the interpretation of the Gaggiano seismic volume and on comparable exhumed structures. M. Mercuri is also grateful to Eni for hosting him for the seismic interpretation of the 3D seismic volume, and to Drs. Andrea D'Ambrosio, Andrea Barrier, Mattia Martinelli, and Fabio La Valle for their technical advice and discussions related to Petrel workflows. We are grateful to Editor Prof. Margaret Rusmore, Associate Editor Prof. Simone Pilia, an anonymous reviewer, and to Prof. Andrea Zanchi for their thoughtful and constructive reviews, which significantly improved the clarity, stratigraphic context, and regional implications of this manuscript. Open access publishing facilitated by Università degli Studi di Roma La Sapienza, as part of the Wiley - CRUI-CARE agreement.

References

Agip. (1987). *Rilievo sismico 3D sulla struttura di Gaggiano*. Internal report, ENI.

Antognini, M., & Bronzini, S. (2018). Foglio 1373 Mendrisio (parte Est) con parte Ovest del foglio Como.—Atlante geologico della Svizzera 1: 25 000, Note esplicative 152.

Argnani, A., & Lucchi, F. R. (2001). Tertiary silicoclastic turbidite systems of the Northern Apennines. In *Anatomy of an orogen: The Apennines and adjacent Mediterranean basins* (pp. 327–349). Springer.

Barbieri, G., & Grandesso, P. (2007). Note Illustrative della Carta Geologica d'Italia. Foglio 082—Asiago.

Bellahsen, N., & Daniel, J. M. (2005). Fault reactivation control on normal fault growth: An experimental study. *Journal of Structural Geology*, *27*(4), 769–780. https://doi.org/10.1016/j.jsg.2004.12.003

Beltrando, M., Stockli, D. F., Decarlis, A., & Manatschal, G. (2015). A crustal-scale view at rift localization along the fossil Adriatic margin of the Alpine Tethys preserved in NW Italy. *Tectonics*, *34*(9), 1927–1951. https://doi.org/10.1002/2015tc003973

Bernoulli, D., Ambrosi, C., Scapozza, C., Castelletti, C., & Wiedenmayer, F. (2017). Foglio 1373 Mendrisio (parte Est) con parte Ovest del foglio Como.—Atlante geologico della Svizzera 1: 25 000, Carta 152.

Berra, F., & Carminati, E. (2010). Subsidence history from a backstripping analysis of the Permo-Mesozoic succession of the Central Southern Alps (Northern Italy). *Basin Research*, *22*(6), 952–975. https://doi.org/10.1111/j.1365-2117.2009.00453.x

Berra, F., Galli, M. T., Reghellin, F., Torricelli, S., & Fantoni, R. (2009). Stratigraphic evolution of the Triassic–Jurassic succession in the Western Southern Alps (Italy): The record of the two-stage rifting on the distal passive margin of Adria. *Basin Research*, *21*(3), 335–353. https://doi.org/10.1111/j.1365-2117.2008.00384.x

Bertotti, G. (1991). Early Mesozoic extension and Alpine shortening in the western Southern Alps: The geology of the area between Lugano and Menaggio (Lombardy, northern Italy). *Memorie di Scienze Geologiche*, *43*, 17–123.

Bertotti, G., Picotti, V., Bernoulli, D., & Castellarin, A. (1993). From rifting to drifting: Tectonic evolution of the South-Alpine upper crust from the Triassic to the Early Cretaceous. *Sedimentary Geology*, *86*(1–2), 53–76. https://doi.org/10.1016/0037-0738(93)90133-p

Bertotti, G., Picotti, V., & Cloetingh, S. (1998). Lithospheric weakening during "retroforeland" basin formation: Tectonic evolution of the central South Alpine foredeep. *Tectonics*, *17*(1), 131–142. https://doi.org/10.1029/97tc02066

Bigi, G., Castellarin, A., Catalano, R., Coli, M., Cosentino, D., Dal Piaz, G. V., et al. (1989). *Synthetic structural-kinematic map of Italy*. C.N.R., Progetto Finalizzato Geodinamica, SELCA Firenze.

Bill, M., O'Dogherty, L., Guex, J., Baumgartner, P. O., & Masson, H. (2001). Radiolarite ages in Alpine-Mediterranean ophiolites: Constraints on the oceanic spreading and the Tethys-Atlantic connection. *GSA Bulletin*, *113*(1), 129–143. https://doi.org/10.1130/0016-7606(2001)113<0129:raiamo>2.0.co;2

Bongiorni, D. (1987). La ricerca di idrocarburi negli alti strutturali mesozoici della Pianura Padana: l'esempio di Gaggiano. *Atti Ticinensi di Scienze della Terra*(31), 125–141.

Bonini, M., Sani, F., & Antonielli, B. (2012). Basin inversion and contractional reactivation of inherited normal faults: A review based on previous and new experimental models. *Tectonophysics*, *522*, 55–88. https://doi.org/10.1016/j.tecto.2011.11.014

Bosellini, A. (1973). Modello Geodinamico e Paleotettonico delle Alpi Meridionali durante il Giurassico—Cretaceo. Sue possibili applicazioni agli Appennini. In B. Accordi (Ed.), *Moderne vedute sulla geologia dell'Appennino*, *Accademia Nazionale dei Lincei* (Vol. 183, pp. 163–205). Atti Convegni.

Butler, R. W., Tavarnelli, E., & Grasso, M. (2006). Structural inheritance in mountain belts: An Alpine–Apennine perspective. *Journal of Structural Geology*, *28*(11), 1893–1908. https://doi.org/10.1016/j.jsg.2006.09.006

Cairo, E., & Ronchi, P. (1995). *Revisione del Triassico della Lombardia centrale. Il rilievo di Gaggiano*. Internal report ENI.

Carcano, C. (1995). *Alto di Gaggiano—Modello di sottosuolo*. Internal report, ENI.

Cardello, G. L., & Doglioni, C. (2015). From mesozoic rifting to Apennine orogeny: The gran Sasso range (Italy). *Gondwana Research*, *27*(4), 1307–1334. https://doi.org/10.1016/j.gr.2014.09.009

Carminati, E., Cavazza, D., Scrocca, D., Fantoni, R., Scotti, P., & Doglioni, C. (2010). Thermal and tectonic evolution of the southern Alps (northern Italy) rifting: Coupled organic matter maturity analysis and thermokinematic modeling. *AAPG Bulletin*, *94*(3), 369–397. https://doi.org/10.1306/08240909069

Carminati, E., & Doglioni, C. (2012). Alps vs. Apennines: The paradigm of a tectonically asymmetric Earth. *Earth-Science Reviews*, *112*(1–2), 67–96. https://doi.org/10.1016/j.earscirev.2012.02.004

Carminati, E., Lustrino, M., & Doglioni, C. (2012). Geodynamic evolution of the central and western Mediterranean: Tectonics vs. igneous petrology constraints. *Tectonophysics*, *579*, 173–192. https://doi.org/10.1016/j.tecto.2012.01.026

Carminati, E., Siletto, G. B., & Battaglia, D. (1997). Thrust kinematics and internal deformation in basement-involved fold and thrust belts: The eastern Orobic Alps case (Central Southern Alps, northern Italy). *Tectonics*, *16*(2), 259–271. https://doi.org/10.1029/96tc03936

Cassano, E. (1986). *Pianura Padana: Interpretazione integrata di dati geofisici e geologici*. Agip.

Castellarin, A., Cantelli, L., Fesce, A. M., Mercier, J. L., Picotti, V., Pini, G. A., et al. (1992). Alpine compressional tectonics in the Southern Alps. Relationships with the N-Apennines. *Annales Tectonicae*, *VI*(1), 62–94.

Castellarin, A., Vai, G. B., & Cantelli, L. (2006). The Alpine evolution of the Southern Alps around the Giudicarie faults: A Late Cretaceous to Early Eocene transfer zone. *Tectonophysics*, *414*(1–4), 203–223. https://doi.org/10.1016/j.tecto.2005.10.019

Chopra, S., & Marfurt, K. J. (2007). *Seismic attributes for prospect identification and reservoir characterization*. Society of Exploration Geophysicists and European Association of Geoscientists and Engineers.

Cuffaro, M., Riguzzi, F., Scrocca, D., Antonioli, F., Carminati, E., Livani, M., & Doglioni, C. (2010). On the geodynamics of the northern Adriatic plate. *Rendiconti Lincei*, *21*(Suppl 1), 253–279. https://doi.org/10.1007/s12210-010-0098-9

Decarlis, A., Beltrando, M., Manatschal, G., Ferrando, S., & Carosi, R. (2017). Architecture of the distal piedmont-Ligurian rifted margin in NW Italy: Hints for a flip of the rift system polarity. *Tectonics*, *36*(11), 2388–2406. https://doi.org/10.1002/2017tc004561

Dercourt, J., Zonenshain, L. P., Ricou, L.-E., Kazmin, V. G., Pichon, X. L., Knipper, A. L., et al. (1986). Geological evolution of the Tethys belt from the Atlantic to the Pamirs since the LIAS. *Tectonophysics*, *123*(1–4), 241–315. https://doi.org/10.1016/0040-1951(86)90199-x

Doglioni, C. (1992a). Relationships between Mesozoic extensional tectonics, stratigraphy and Alpine inversion in the Southern Alps. *Eclogae Geologicae Helvetiae*, *1*(85), 105–126.

Doglioni, C. (1992b). The Venetian Alps thrust belt. In *Thrust tectonics* (pp. 319–324). Springer.

Fantoni, R., Bersezio, R., & Forcella, F. (2004). Alpine structure and deformation chronology at the Southern Alps-Po Plain border in Lombardy. *Bollettino della Societa Geologica Italiana*(123), 463–476.

Fantoni, R., Bersezio, R., Forcella, F., Gorla, L., Mosconi, A., & Picotti, V. (1999). New dating of the Tertiary magmatic products of the central Southern Alps, bearings on the interpretation of the Alpine tectonic history. *Memorie di Scienze Geologiche*, *1*(51), 47–61.

Fantoni, R., & Franciosi, R. (2010). Tectono-sedimentary setting of the Po Plain and Adriatic foreland. *Rendiconti Lincei*, *21*(Suppl 1), 197–209. https://doi.org/10.1007/s12210-010-0102-4

Fantoni, R., & Scotti, P. (2003). Thermal record of the Mesozoic extensional tectonics in the Southern Alps. *Atti Ticinensi di Scienze della Terra*, 96–101.

Ferrando, S., Bernoulli, D., & Compagnoni, R. (2004). The Canavese zone (internal Western Alps): A distal margin of Adria. *Schweizerische Mineralogische und Petrographische Mitteilungen*, *84*(1–20), 237–259.

Ghielmi, M., Minervini, M., Nini, C., Rogledi, S., & Rossi, M. (2013). Late Miocene–Middle Pleistocene sequences in the Po Plain—Northern Adriatic Sea (Italy): The stratigraphic record of modification phases affecting a complex foreland basin. *Marine and Petroleum Geology*, *42*, 50–81. https://doi.org/10.1016/j.marpetgeo.2012.11.007

Ghielmi, M., Minervini, M., Nini, C., Rogledi, S., Rossi, M., & Vignolo, A. (2010). Sedimentary and tectonic evolution in the eastern Po-Plain and northern Adriatic Sea area from Messinian to Middle Pleistocene (Italy). *Rendiconti Lincei*, *21*(Suppl 1), 131–166. https://doi.org/10.1007/s12210-010-0101-5

Handy, M. R., Schmid, S. M., Bousquet, R., Kissling, E., & Bernoulli, D. (2010). Reconciling plate-tectonic reconstructions of Alpine Tethys with the geological–geophysical record of spreading and subduction in the Alps. *Earth-Science Reviews*, *102*(3–4), 121–158. https://doi.org/10.1016/j.earscirev.2010.06.002

Harris, C. R., Millman, K. J., van der Walt, S. J., Gommers, R., Virtanen, P., Cournapeau, D., et al. (2020). Array programming with NumPy. *Nature*, *585*(7825), 357–362. https://doi.org/10.1038/s41586-020-2649-2

Holdsworth, R. E., Butler, C. A., & Roberts, A. M. (1997). The recognition of reactivation during continental deformation. *Journal of the Geological Society*, *154*(1), 73–78. https://doi.org/10.1144/gsjgs.154.1.0073

Hunter, J. D. (2007). Matplotlib: A 2D graphics environment. *Computing in Science & Engineering*, *9*(3), 90–95. https://doi.org/10.1109/MCSE.2007.55

Lescoutre, R., & Manatschal, G. (2020). Role of rift-inheritance and segmentation for orogenic evolution: Example from the Pyrenean-Cantabrian system. *Bulletin de la Societe Geologique de France*, *191*(1), 18. https://doi.org/10.1051/bsgf/2020021
Livani, M., Scrocca, D., Arecco, P., & Doglioni, C. (2018). Structural and stratigraphic control on salient and recess development along a thrust belt front: The Northern Apennines (Po Plain, Italy). *Journal of Geophysical Research: Solid Earth*, *123*(5), 4360–4387. https://doi.org/10.1002/2017jb015235
Mariotti, G., & Doglioni, C. (2000). The dip of the foreland monocline in the Alps and Apennines. *Earth and Planetary Science Letters*, *181*(1–2), 191–202. https://doi.org/10.1016/s0012-821x(00)00192-8
McKinney, W. (2010). Data structures for statistical computing in Python. In *Proceedings of the 9th Python in Science Conference* (pp. 51–56).
Mohn, G., Manatschal, G., Masini, E., & Müntener, O. (2011). Rift-related inheritance in orogens: A case study from the Austroalpine nappes in Central Alps (SE-Switzerland and N-Italy). *International Journal of Earth Sciences*, *100*(5), 937–961. https://doi.org/10.1007/s00531-010-0630-2
Morley, C. K. (2017). The impact of multiple extension events, stress rotation and inherited fabrics on normal fault geometries and evolution in the Cenozoic rift basins of Thailand. *Special Publication*, *439*(1), 413–445. https://doi.org/10.1144/sp439.3
Pace, P., Scisciani, V., Calamita, F., Butler, R. W., Iacopini, D., Esestime, P., & Hodgson, N. (2015). Inversion structures in a foreland domain: Seismic examples from the Italian Adriatic Sea. *Interpretation*, *3*(4), SAA161–SAA176. https://doi.org/10.1190/int-2015-0013.1
Pieri, M., & Groppi, G. (1981). *Subsurface geological structure of the Po Plain, Italy (Consiglio Nazionale delle Ricerche—Progetto finalizzato geodinamica sottoprogetto "Modello strutturale")*. Agip.
Prosser, G. (1998). Strike-slip movements and thrusting along a transpressive fault zone: The North Giudicarie Line (Insubric Line, northern Italy). *Tectonics*, *17*(6), 921–937. https://doi.org/10.1029/1998TC900010
Rocca, M., Zanchetta, S., Gasparrini, M., Mangenot, X., Berra, F., Deschamps, P., et al. (2024). U-Pb carbonate dating reveals long-lived activity of proximal margin extensional faults during the Alpine Tethys rifting. *Terra Nova*, *36*(5), 347–357. https://doi.org/10.1111/ter.12717
Rocca, M., Zanchetta, S., & Zanchi, A. (2026). Inherited rift faults as drivers of orogenic complexity: The case of the Amora Fault System, central Southern Alps (N Italy). *Journal of Structural Geology*, *205*, 105650. https://doi.org/10.1016/j.jsg.2026.105650
Scaramuzzo, E., Livio, F. A., Granado, P., Di Capua, A., & Bitonte, R. (2022). Anatomy and kinematic evolution of an ancient passive margin involved into an orogenic wedge (Western Southern Alps, Varese area, Italy and Switzerland). *Swiss Journal of Geosciences*, *115*(1), 4. https://doi.org/10.1186/s00015-021-00404-7
Schönborn, G. (1992). Kinematics of a transverse zone in the Southern Alps, Italy. In *Thrust tectonics* (pp. 299–310). Springer.
Schumacher, M. E., Schönborn, G., Bernoulli, D., & Laubscher, H. P. (1997). Rifting and collision in the southern Alps. In O. Pfiffner, P. Lehner, P. Heitzmann, S. Mueller, & A. Steck (Eds.), *Structure of the Swiss Alps: Results from the National Research Program 20 (NFP 20)*, *Deep* (pp. 186–204). Birkhäuser.
Scisciani, V. (2009). Styles of positive inversion tectonics in the Central Apennines and in the Adriatic foreland: Implications for the evolution of the Apennine chain (Italy). *Journal of Structural Geology*, *31*(11), 1276–1294. https://doi.org/10.1016/j.jsg.2009.02.004
Seabold, S., & Perktold, J. (2010). Statsmodels: Econometric and statistical modeling with python. In *Proceedings of the 9th Python in Science Conference*.
Sieberer, A.-K., Willingshofer, E., Klotz, T., Ortner, H., & Pomella, H. (2023). Inversion of extensional basins parallel and oblique to their boundaries: Inferences from analogue models and field observations from the Dolomites Indenter, European eastern Southern Alps. *Solid Earth*, *14*(7), 647–681. https://doi.org/10.5194/se-14-647-2023
Tavani, S., Granado, P., Corradetti, A., Camanni, G., Vignaroli, G., Manatschal, G., et al. (2021). Rift inheritance controls the switch from thin- to thick-skinned thrusting and basal décollement re-localization at the subduction-to-collision transition. *GSA Bulletin*, *133*(9–10), 2157–2170. https://doi.org/10.1130/b35800.1
Tavarnelli, E., Butler, R. W. H., Decandia, F. A., Calamita, F., Grasso, M., Alvarez, W., et al. (2004). Implications of fault reactivation and structural inheritance in the Cenozoic tectonic evolution of Italy. In *The geology of Italy, special* (Vol. 1, pp. 209–222).
Turrini, C., Bosica, B., Ryan, P., Shiner, P., Lacombe, O., & Roure, F. (2018). 3D structural and thermal modelling of Mesozoic petroleum systems in the Po Valley Basin, northern Italy. *Petroleum Geoscience*, *24*(2), 172–196. https://doi.org/10.1144/petgeo2017-031
Turrini, C., Lacombe, O., & Roure, F. (2014). Present-day 3D structural model of the Po Valley basin, Northern Italy. *Marine and Petroleum Geology*, *56*, 266–289. https://doi.org/10.1016/j.marpetgeo.2014.02.006
Turrini, C., Toscani, G., Lacombe, O., & Roure, F. (2016). Influence of structural inheritance on foreland-foredeep system evolution: An example from the Po valley region (northern Italy). *Marine and Petroleum Geology*, *77*, 376–398. https://doi.org/10.1016/j.marpetgeo.2016.06.022
Vitale, S., Amore, O. F., Ciarcia, S., Fedele, L., Grifa, C., Prinzi, E. P., et al. (2018). Structural, stratigraphic, and petrological clues for a Cretaceous–Paleogene abortive rift in the southern Adria domain (southern Apennines, Italy). *Geological Journal*, *53*(2), 660–681. https://doi.org/10.1002/gj.2919
Vitale, S., & Ciarcia, S. (2022). The dismembering of the Adria platforms following the Late Cretaceous-Eocene abortive rift: A review of the tectono-stratigraphic record in the southern Apennines. *International Geology Review*, *64*(20), 2866–2889. https://doi.org/10.1080/00206814.2021.2004559
Waskom, M. L. (2021). Seaborn: Statistical data visualization. *Journal of Open Source Software*, *6*(60), 3021. https://doi.org/10.21105/joss.03021
Weert, A., Camanni, G., Mercuri, M., Ogata, K., Vinci, F., & Tavani, S. (2025). Displacement analysis of basin-scale reactivated normal faults: Insights from the West Netherlands Basin. *Journal of Structural Geology*, *192*, 105356. https://doi.org/10.1016/j.jsg.2025.105356
Winterer, E. L., & Bosellini, A. (1981). Subsidence and sedimentation on Jurassic passive continental margin, Southern Alps, Italy. *AAPG Bulletin*, *65*(3), 394–421. https://doi.org/10.1306/2f9197e2-16ce-11d7-8645000102c1865d
Zampieri, D. (1995). Tertiary extension in the southern Trento Platform, Southern Alps, Italy. *Tectonics*, *14*(3), 645–657. https://doi.org/10.1029/94tc03093
Zanchetta, S., Garzanti, E., Doglioni, C., & Zanchi, A. (2012). The Alps in the Cretaceous: A doubly vergent pre-collisional orogen. *Terra Nova*, *24*(5), 351–356. https://doi.org/10.1111/j.1365-3121.2012.01071.x
Zanchi, A., D'Adda, P., Zanchetta, S., & Berra, F. (2012). Syn-thrust deformation across a transverse zone: The Grem–Vedra fault system (central Southern Alps, N Italy). *Swiss Journal of Geosciences*, *105*(1), 19–38. https://doi.org/10.1007/s00015-011-0089-6